FINNISH ROAD ADMINISTRATION

Leena Korkiala-Tanttu, Rainer Laaksonen, Jouko Törnqvist

Effect of spring and overload on the rutting of a low-volume road

HVS-Nordic - research

Finnra Reports 22/2003

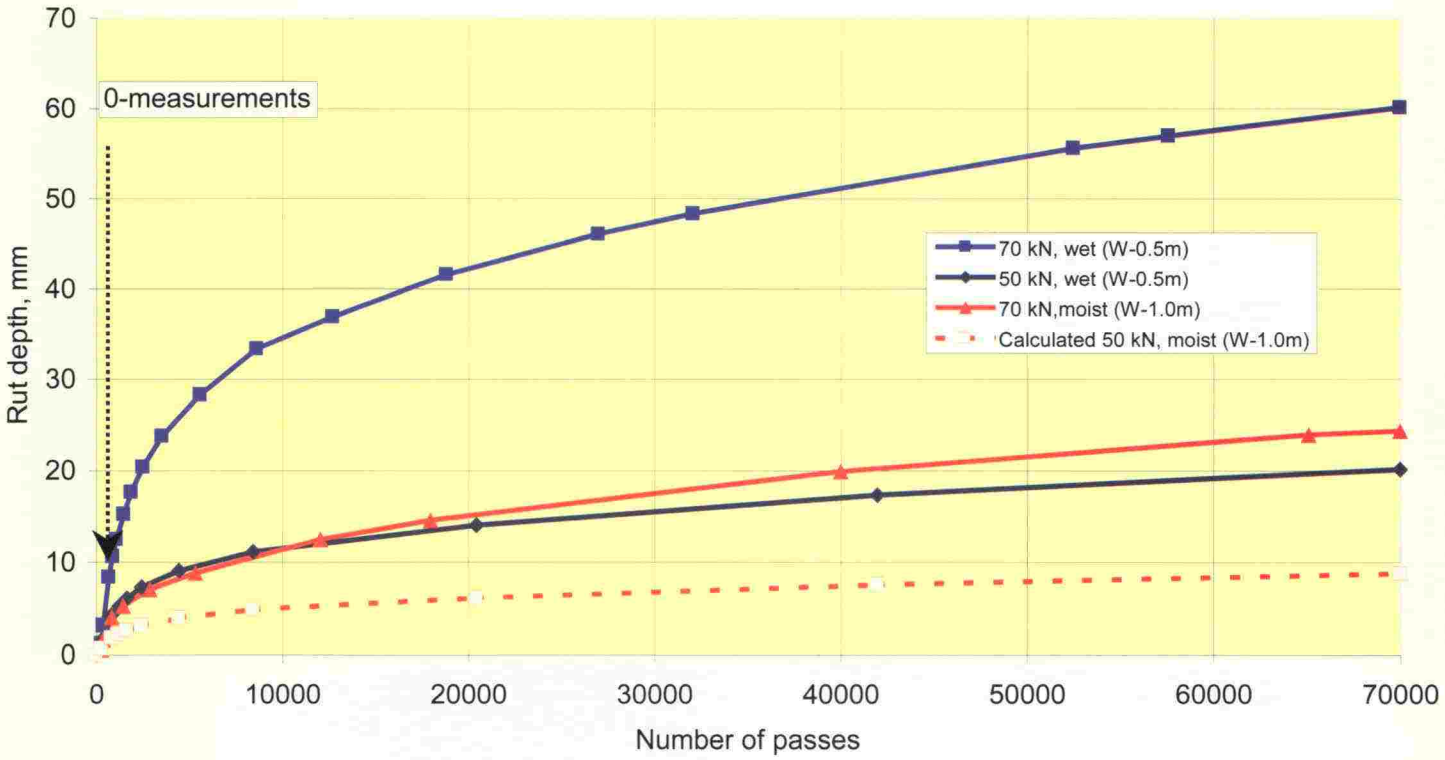

Leena Korkiala-Tanttu, Rainer Laaksonen, Jouko Törnqvist

Effect of spring and overload on the rutting of a low-volume road

HVS-Nordic - research

Finnra Reports 22/2003

FINNRA
Helsinki 2003

ISSN 1457-9871
ISBN 951-803-052-9
TIEH 3200810E

Internet (pdf) : www.tiehallinto.fi/julkaisut
ISSN 1459-1553
ISBN 951-803-053-7
TIEH 3200810E-v

Edita Prima Oy
Helsinki 2003

This publication is available at:
Finnra Publications Sales
fax int. +358 204 22 2652
e-mail julkaisumyynti@tiehallinto.fi

Finnish Road Administration
Opastinsilta 12 A
PB 33
FIN-00521 HELSINKI
Phone int. +358 204 22 11

Leena KORKIALA-TANTTU, Rainer LAAKSONEN, Jouko TÖRNQVIST: Effect of the spring and overload to the rutting of a low-volume road. HVS-Nordic-research. Helsinki 2003. Finnish Road Administration. Finnra Reports 22/2003. 39 p. + app. ISSN 1457-9871, ISBN 951-803-052-9, TIEH 3200810E.

Keywords: low-volume roads, accelerated pavement test, rutting, permanent deformation

ABSTRACT

The research is part of the development of the economical maintenance of low-volume roads. The research concentrates on the behaviour of pavement with low bearing capacity under spring conditions and overload. Finnish Road Administration Finnra financed the research.

The tested structures consisted of three similar structures. The tests were carried out using a Heavy Vehicle Simulator (HVS). Axle load and spring conditions (water level) were varied from test to test. In all, there were two different axle loads (50 kN and 70 kN) and two different water levels (depths 0.5 m and 1.0 m from the asphalt surface). With the upper water level both 50 kN and 70 kN axle loads were tested. With the lower water level only the 70 kN load was tested. The structures were constructed in January - February 2002 and tested in February - April 2002.

The objective of the research was to study the validity of the 'fourth power rule' on rutting under spring conditions. It makes it possible to evaluate the effect of the possible increase of axle loads on the performance of low-volume roads. It also makes it possible to evaluate the traffic volume above which single overloads dictate the design of the road construction. One other objective is to ascertain how big a part spring plays in the damage process.

The structures tested were constructed in Otaniemi in the test basin with rock walls and sand subgrade. The structures tested represent low-volume road structures. The total thickness of the structures was 500 mm, consisting of 50 mm asphalt concrete, 200 mm crushed rock and 250 mm crushed gravel. The crushed gravel fulfilled the grain size requirements, but not the requirements of the specific surface area.

The construction work was carefully done to achieve even and uniform quality construction layers. The evenness of the layers was good except for the asphalt layer. It was difficult to construct and compact materials in a relatively narrow basin. The measured bearing capacities were clearly under the requirements of Finnra for low-volume roads. All structures became more compact during the testing. The constructions were insulated from the frost during the construction and testing time.

The instrumentation of the structures was designed to measure both the dynamic and permanent vertical displacements in each layer. The test wheel was a dual wheel with two axle loads. To be able to repeat the tests and interpret them, spring conditions were simulated through two different water levels.

There was only a slight upheaval alongside the ruts and the bearing capacities of each structure increased during the tests. Therefore, the permanent deformations of the structures seem to be mostly compaction. No notable damage - in spite of the deep rut depths - was detected.

The rutting of the structures was monitored by profilometer measurements. An additional calculation was made to find how much a similar structure would be rutted under an axle load of 50 kN and with a lower water level. The rutting results were also fixed to correspond to a situation with the same thickness of the asphalt concrete. The results were then compared together. According to the results, the depth of the rut grew 2.8 - 3 times bigger when the axle load was raised from 50 kN to 70 kN. Raising the water level 500 mm speeds up the rutting 2.2 - 2.5 times. When both the water level and axle load was raised, the depth of the rut was 5.5 - 6.0 times bigger. It was also noticed that the width of the rutting area depends on its depth. The width of the rut is greatest when the rut is deepest.

The water content of the structure before and after the changes in water level was monitored by radiometric measurements. The water content in the unbound layers above the water level rose about 0.2 - 0.5% units when the water level was raised 500 mm. The change is small, yet it greatly influences the rate of rutting.

Many instruments (Emu-Coils, settlement profile tubes and thickness gauges) were used for monitoring the permanent deformations in different layers. All measurements showed the same features: most of the rutting (about 47 - 59%) happened in the subgrade (sand). The proportion of the rutting of the asphalt was 3.5 - 6%, the crushed rock 15 - 23% and the crushed gravel 23 - 27%. When the upper level of the water was on the surface of the subgrade, deformations were bigger in the subgrade and in the crushed gravel. When the water was at its lower level, a relatively greater proportion of the deformations happened in the upper parts of the structure.

A clear growth in the deformations of all the materials was detected once the elastic deformations corresponding to a certain stress state had crossed a particular threshold value. This means that the 'shakedown' value was crossed.

The structural damage can be estimated by using the empirical 'fourth power rule'. This rule assumes that the fourth power of the relation of the axle loads can be used to estimate the growth in the damage. The HVS tests carried out by VTT show that this rule is not valid for estimating the rutting rate of low-volume roads. It is only valid when the traffic volume is very small; in this case 200 - 450 passes. Beyond this, the permanent deformations begin to govern the behaviour.

The earth pressure in the subgrade was monitored during the tests. By using the pressure and deformation results, a back-calculation was made to find out what had been the real resilient moduli. These calculated moduli were compared with the laboratory results. The back-calculated moduli were 15 - 40% smaller than those of the laboratory tests. Contrary to expectations, the resilient modulus was the smallest in the case of the biggest load and lower water level.

During the tests, a great deal of data were recorded. In this research, the data were analysed and studied only within the objectives of the research. The data will be studied more carefully in future research.

FOREWORD

"Effect of spring and overload on the rutting of a low-volume road" is a heavy vehicle simulator study financed by Finnish Road Administration Finnra. It is part of a project to develop economical maintenance of low-volume roads and focuses on the behaviour of roads with low bearing capacity. The study complements the low-volume road structures project. The study was carried out by VTT Building and Transport under the supervision of Finnra according to a research plan.

The aim of the study was to acquire basic information on the behaviour of road structures with low bearing capacity. The study also aimed at discovering whether the fourth power rule is valid, as well as the effect of spring on for low-volume roads. It also studied the effect of spring under a Heavy Vehicle Simulator (HVS) load imitating the passing of a lorry.

The research was carried out by VTT Building and Transport. Markku Tuhola and Jari Pihlajamäki prepared the testing programme and its financing. Jouko Törnqvist and Leena Korkiala-Tanttu were responsible for the more detailed planning of the study and analysing the results. Construction, instrumentation and loading the structures was carried out by Pekka Halonen and Janne Sikiö. Janne Sikiö drew up the design and instrumentation drawings of the test sites. Rainer Laaksonen was responsible for laboratory tests and their reporting. The sub-tasks were compiled and analysed and the report written by Leena Korkiala-Tanttu.

Espoo, February 2003

VTT Building and Transport

Contents

1 GENERAL DESCRIPTION OF THE TEST BASIN AND LOADING

1.1 Test basin

There are two test basins in Otaniemi for Heavy Vehicle Simulator (HVS) loading tests. One basin is made of concrete and the other is extracted in rock. The structures studied were constructed in the basin with rock walls (Figures 1.1 and 1.2). The top of the rock basin is level with the surface of the ground. The average depth of the basin is 2.0 m and its total length is approximately 40 m, including the ramp at one end. The basin's bottom and walls are waterproofed with urethane and the water level can be regulated with water from the municipal water distribution system. A tent providing protection from the elements is erected above the basin.

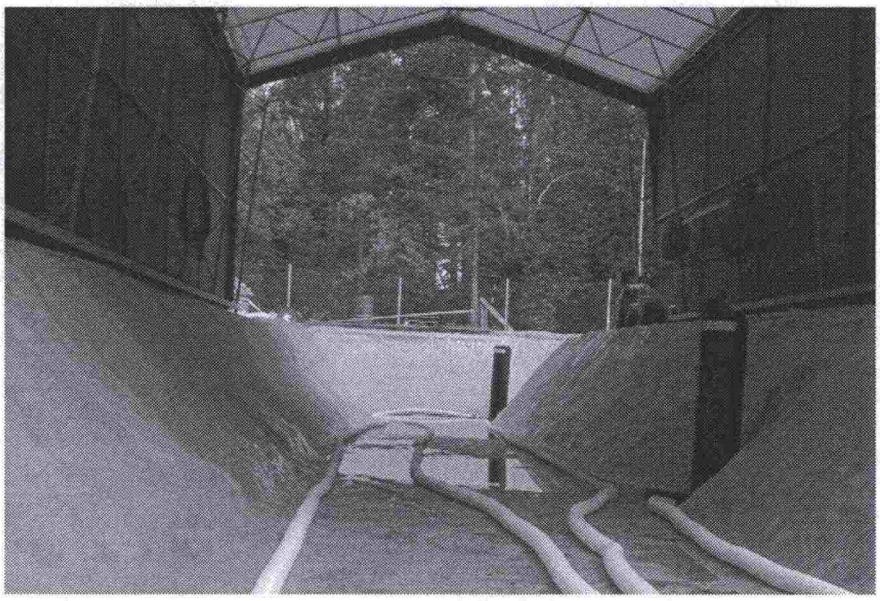

Kuva 1.1. The empty rock basin.

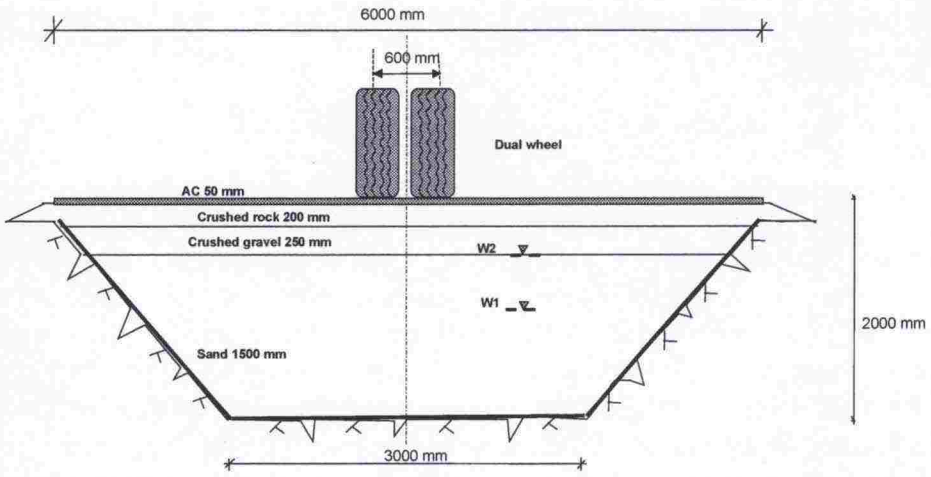

Figure 1.2. Cross section of the structure.

1.2 Load with Heavy Vehicle Simulator (HVS)

The Heavy Vehicle Simulator (HVS) is 23 m long, 3.7 m wide, 4.2 m high and its total mass is 46 metric tons (Fig 1.3). The maximum width of HVS's loading area is 1.5 m. The total length of the loading area is eight metres, of which six metres can be used with even wheel load and speed. At either end of the loading area, a distance of one metre is necessary for accelerating and braking the wheel, and, in one-way application of load, for lowering and lifting the wheel to and from the surface. The speed of the wheel can be adjusted between 1 to 15 km/h. However, in long-term loading, the maximum speed is 12 km/h. Any distribution with 50 millimetre lateral adjustments can be selected as the lateral movement of the test wheel. The load can be applied either one-way or in both directions.

The maximum load achieved with the simulator is 110 kN and the minimum 25 to 30 kN. The load can be applied on the structure via either a lorry single tyre or twin tyre. The simulator includes a heating/cooling unit for keeping the road structure to be tested at the desired temperature. In this test, the temperature was +10 □C.

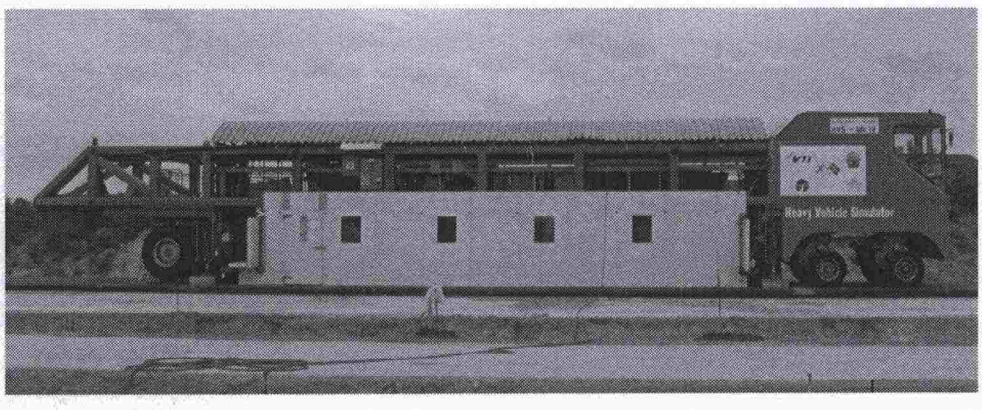

Figure 1.3. HVS-Nordic, Heavy Vehicle Simulator.

2 CONSTRUCTION

2.1 Structure

The test structure was built in VTT's rock basin in Otaniemi, Espoo. The structure was the same on all sections to be tested. The total thickness of the pavements was 500 mm. The structure chosen corresponds to the pavements of low-volume roads.

Before constructing the test structure, old test structures were removed from the basin as far as the surface of the subgrade layer. Thus, the subgrade consisted of fine to medium sand that had been in the bottom of the previous test structure.

The subbase consisted of so-called low-grade crushed gravel with grain size 0 to 35 mm and the thickness of the layer was 250 mm. The base course was made of crushed rock from Teisko, with a grain size 0 to 32 mm and thickness 200 mm. The asphalt consisted of a 50 mm layer of asphalt (AC16/125, B70/100). The pavements are shown in Figure 2.1.

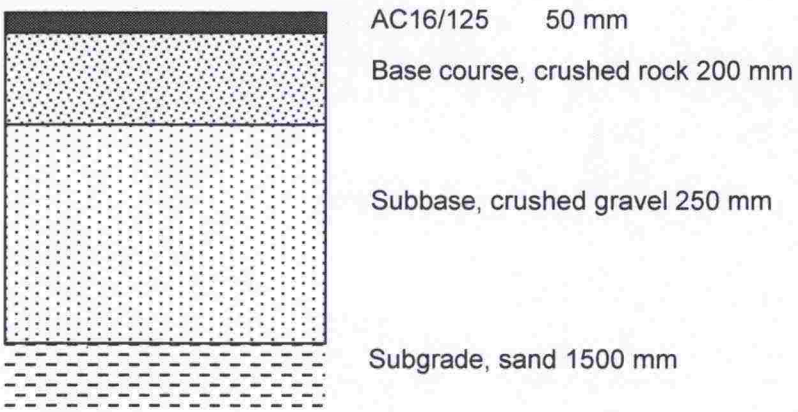

Figure 2.1. Pavements.

2.2 Construction

The test structure was constructed in January and February 2002. The work began by thawing the top part of the subgrade. The construction work was carried out in such a way that the structure was not allowed to freeze during the construction or testing period, at least not in the area to be loaded. The intrusion of frost the structure during the various phases was prevented by thermal insulation and warm air blowers.

The subgrade sand was levelled and compacted and instruments were installed. The lower layer of the pavement was constructed from crushed gravel, which was brought from Jutikkala. The thickness of the layer when compacted was approximately 250 mm. Due to winter working conditions,

the material was not watered during compaction. The compacted layer was instrumented and samples were taken from it.

Crushed rock from previous test structures was used as the crushed rock material in the base course. As with the crushed gravel layer, compaction was carried out as a single layer without watering. The compacted layer was instrumented and samples were taken from it. The quality of work on the unbound layers was monitored with Loadman, falling weight deflectometer, sand cone volumeter and Troxler measurements, as well as levelling. Because the layers were built and the instruments installed outdoors in the winter, the whole structure was carefully insulated after each shift.

The bound layer was made of asphalt concrete. The quality of the work was monitored with levelling, as well as Loadman and falling weight deflectometer measurements. Finally, the layer was instrumented. The evenness of the layer was measured with DOR measurements conducted after the testing.

The basic water table level during the first two tests was the bottom of the subbase (W2), later referred to as wet conditions. During the last test, the water table level was lowered to approximately 1000 mm from the top of the asphalt (W1), later referred to as moist conditions.

Testing began at the beginning of March. The structures were tested in the following order: structure 22 (50 kN, wet), structure 21 (70 kN, wet) and finally structure 23 (70 kN, moist). Figure 2.2 shows the loading schedule and the changes in the water table level.

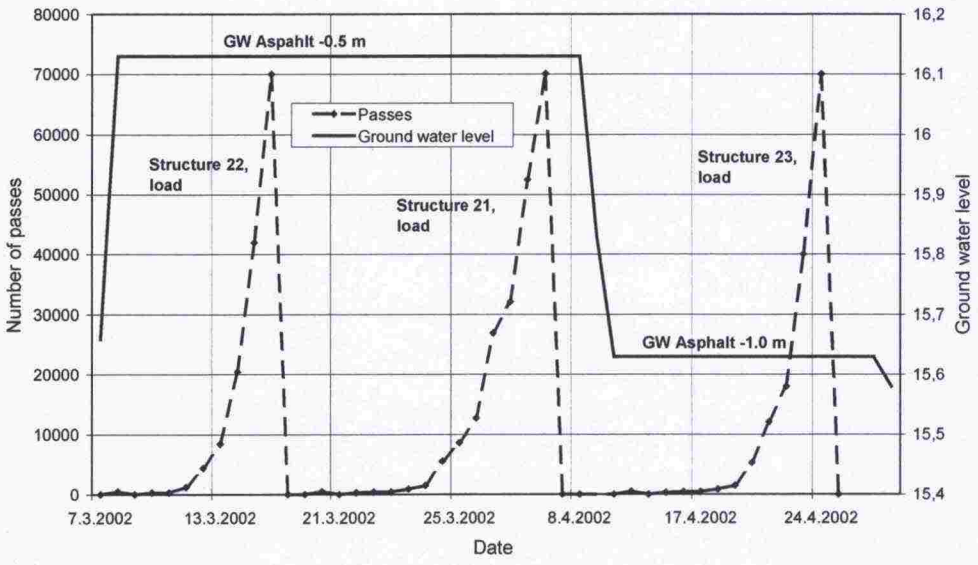

Figure 2.2. Loading the structures and level of ground water measured in the pilot well

3 INSTRUMENTATION

The objective of the instrumentation was to monitor and measure deformations and changes in moisture and temperature occurring in the structure. Structural deformations, earth pressures and the water content of the layers were measured during loading. The responses recorded in the measurements were both dynamic and static.

Some of the instruments were installed after the test structure was built. Sensors for measuring earth pressure and displacements were installed during the construction. The sensors were calibrated and installed carefully following instrument-specific instructions. The test structures were also equipped with instruments related to a deformation project (settlement profile tubes and aluminium foil).

Post-construction instrumentation consisted of instruments and their installation tubes measuring temperature, water content in the structures and asphalt deflection. Asphalt deflection was measured with an accelerometer, which was installed in each structure immediately prior to the test beginning.

Figure 3.1 shows the numbering of the test sections, loads and water table levels. Appendix 1 presents more detailed maps, longitudinal profiles and a cross section of the structures. These drawings illustrate the positions of the instruments, the geometric characteristics of the structure and loading areas.

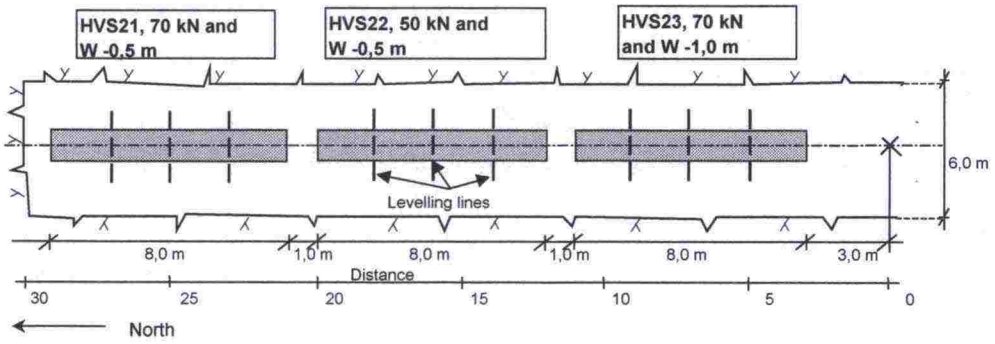

Figure 3.1. The dimensions and numbering of test sections

4 TESTING PROGRAMME AND MEASUREMENT RESULTS

4.1 *In-situ* measurements

The purpose of tests and measurements conducted on the test structures and materials before and during construction was to study the properties of the test structure materials and verify the functioning of the materials in the structures. The tests also formed part of the quality control of the test structures.

During HVS testing, the objective of the measurements was to study earth pressures and water content present in the structure, as well as displacements in the parts of the structure critical to deformation.

Measurements after the testing aimed at discovering variation in the bearing capacity of the structure as seasons and conditions change, as well as deformations occurring in different layers of the structure under strain.

4.1.1 Falling weight deflectometer measurements

Falling weight deflectometer (FWD) measurements were conducted on top of the crushed rock and the asphalt immediately after the structure in question was built. In the beginning of testing, before the HVS was moved to the test site, the bearing capacity of the structures was measured for both water table levels (W1 and W2). The results for the measurements during construction are given in Appendix 2.

4.1.2 Radiometric measurements

Radiometric measurements on each test section were conducted for two water table levels before and after testing. In addition, measurements were carried out on each section a couple of months after the testing ended, when the water table was well below the –1.0 meter level (Appendix 2).

4.1.3 Instrumentation, levelling and density measurements.

The surface of each layer was levelled before constructing the next layer. The vertical positions of the instruments were also verified by levelling. The results of levelling and density measurements are presented in Appendix 2.

4.2 Laboratory tests and sampling

The laboratory tests of unbound materials consisted of determining the grain size distribution and compactibility, as well as resilient modulus and strength tests. The deformation properties of the materials were not established.

The unbound materials used in the tests were sand, crushed gravel and crushed rock. The subgrade consisted of sand, the subbase of crushed gravel (#0–35 mm). The grain size distribution of the sand corresponded to fine to medium sand. The quality of the crushed gravel was slightly below average, as its specific surface area was 4.36 m^2/g (PANK 2401). The base course consisted of crushed rock (#0–32 mm). The properties of the materials are described in more detail in /Törnqvist & Jauhiainien 2001/. Grains of over 32 mm were removed from the crushed rock and crushed gravel before the tests. The grading curves of the materials are presented in Figure 4.1.

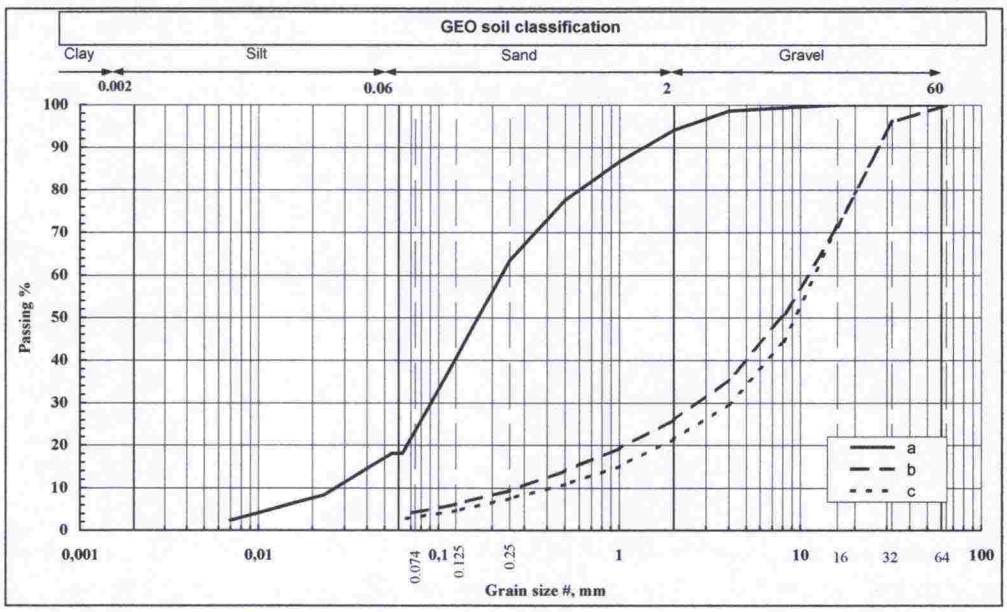

Figure 4.1. The grading curves of the materials studied (a = sand, b = crushed gravel, c = crushed rock).

Improved Proctor tests were conducted on sand, crushed gravel and crushed rock to determine maximum dry bulk density and optimum water content. The results are presented in Table 4.1. The results of the Proctor tests are presented in Appendix 3.

Table 4.1. The results of the Proctor tests on the materials studied.

Material	Maximum dry bulk density / -dry density (g/cm^3 / kN/m^3)	Optimum water content (%)
Sand	1.91 / 18.7	10.4
Crushed gravel	2.35 / 23.1	5.6
Crushed rock	2.14 / 21.0	5.0

Resilient modulus tests

The tests were conducted according to the SHRP P46 protocol and partly expanding on it. The objective was to obtain a clear picture of the variation in the stiffness of the material in different stress states. A sample cylinder with a 152 mm diameter (D) and 300 mm height (H) was used in the tests. The condition variables of the materials (density and water content) were chosen on the basis of the Proctor tests and density measurements of the structure (volumeter, Troxler). The optimum water content – 2 percentage units – was chosen as the test's water content. The densities, water contents and degrees of compaction in the samples before the test are given in Table 4.2.

Table 4.2. The condition variables of the materials realised in the modulus tests (in the beginning).

Material	Dry bulk density (g/cm^3)	Water content (%)	Degree of compaction (%)
Sand	1.80	8.36	94.1
Sand (2)	1.80	8.35	94.4
Crushed gravel	2.22	3.03	94.3
Crushed rock	2.10	2.89	97.8

The test results were used for calculating a resilient modulus for each material and load step. Resilient moduli were determined for each material in 21 different stress states. The results are presented in Figure 4.2.

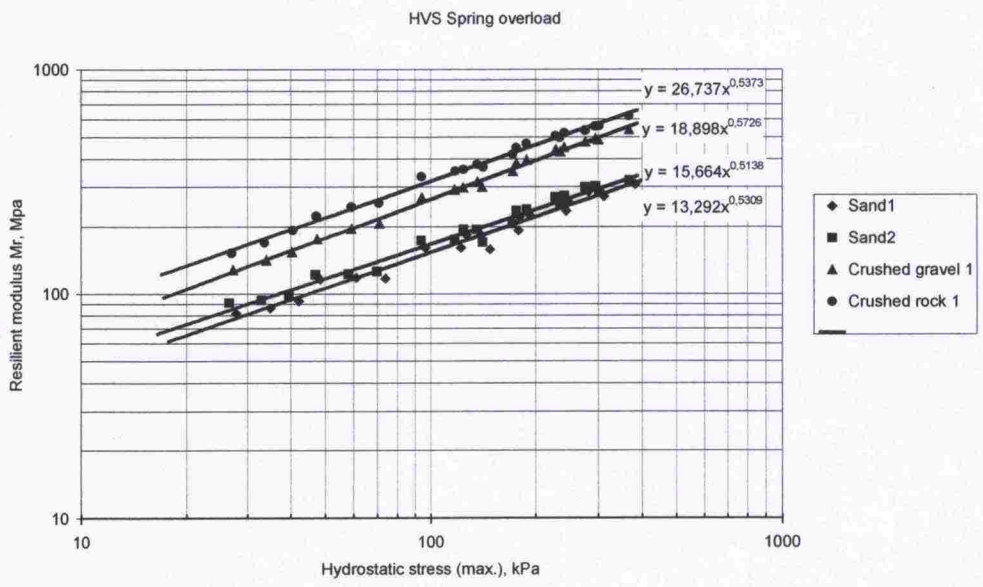

Figure 4.2. Modulus tests. The resilient modulus values for various materials in the stress states used.

Determining the resilient moduli with the SHRP P46 method was successful for all the materials. For sand, the stiffness level was lower than observed in earlier studies. The stiffness of crushed rock was also lower than the stiffness of earlier samples analysed. The stiffness level of crushed gravel corresponded to the values defined for crushed gravel in the Road Structures Research Programme, TPPT.

Strength tests

The tests were conducted on one sample using a multi-stage testing procedure. In this method, the sample is loaded until failure on one confining pressure, after which the confining pressure is increased and the sample is again loaded until failure. The tests in the series were conducted on four confining pressures: 10, 20, 40 and 80 kPa.

During the test, in addition to force, vertical and horizontal deformations were measured in the sample, so that stresses could be calculated as accurately as possible for the duration of the entire strength test. The condition variables for the materials were the same as for the modulus tests. The densities, water contents and degrees of compaction in the samples before the test are given in Table 4.3.

Table 4.3. The condition variables of the materials in the strength tests (in the beginning).

Material	Dry bulk density (g/cm^3)	Water content (%)	Degree of compaction (%)
Sand	1.81	8.39	94.5
Crushed gravel	2.22	2.89	94.5
Crushed rock	2.14	2.90	99.6

The confining pressure (σ_3) – shear strength (τ) points determined from the test results are presented in Figure 4.4. An angle of friction and cohesion were determined from the results of each strength test. Due to the method used, the strength parameters determined represent critical state strength rather than the maximum strength of the material. Examining the test results also shows that the first point does not fit into the pattern – the test was not continued sufficiently long. The development of strength was non-linear in the stress range used (10 - 80 kPa).

The strength parameters interpreted from the test results are collected in Table 4.4. The interpretation ignores the test stage conducted with confining pressure 10 kPa (Figure 4.4). Determining the strength parameters with the new multi-stage test was reasonably successful. The tests produced the anticipated results for the strength parameters.

Table 4.4. Strength parameters for different materials.

Material	Angle of friction (°)	Cohesion (kPa)
Sand	35.5	12.9
Crushed gravel	44.7	35.6
Crushed rock	43.1	43.0

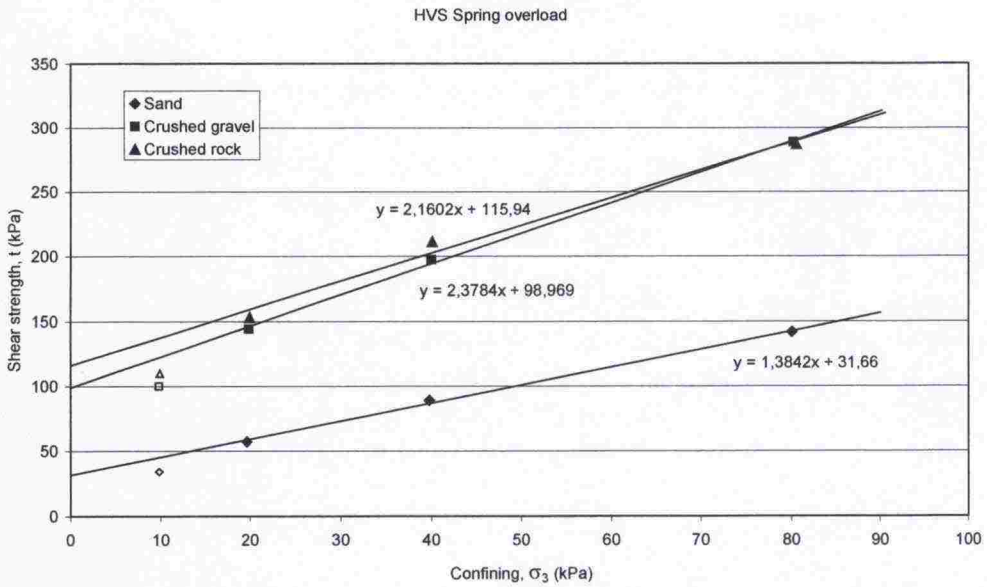

Figure 4.3. Strength tests. Determining strength parameters on confining pressure – shear strength axes.

4.3 Deformation study measurements

The measurements related to the deformation study were conducted according to a separate plan at the beginning and end of testing. They included both settlement profile and eddy-current measurements. The objective of the measurements was to determine the reliability of different measuring methods and how well they can be applied to determining permanent deformations in different layers. The results are presented in a separate report /Kivikoski & Laaksonen 2002/.

4.4 Loading and condition parameters of the test

The heavy vehicle simulator was moved to the structure on 26 February 2002, when the ground water level had stabilised at about one metre from the top surface. Testing the sections began with the middle section (structure 22), structure 21 was tested next and structure 23 last. A dual wheel was chosen as the loading wheel, the loading was carried out in two directions and the loading speed was 12 km/h. On structure 22, the wheel load used was 50 kN and the ground water level was at the bottom of the sub-

base (depth from the asphalt surface – 0.5 m). The tyre pressure for the 50 kN load was 700 kPa. On structures 21 and 23 the load used was 70 kN and tyre pressure 850 kPa. The ground water level for structure 21 was still maintained at the bottom of the subbase. In the last test (structure 23) the ground water level was lowered to one metre from the top of the asphalt.

Efforts were made to keep the water table level constant during the testing of different loading sections. The loading areas of the structures were not allowed to freeze after the construction. The temperature of the structures during loading was + 10□C.

The loading distribution in the tests had 100 mm intervals between load positions (Table 4.5). Earth pressure and deformation measurements were conducted when the load was positioned directly in the centre and in the extreme right position. Rut measurements were always conducted at the same stage of loading, that is, the position of the dual wheel was always the same when conducting measurements.

After initial measurements, the load was increased with 10 kN intervals until the actual load level was reached. After that the measuring interval was distributed so that measurements could be conducted during rut formation, first at 1.5 mm and finally at 3.0 mm intervals.

Table 4.5. Loading programme

Number of load repetitions	Wheel load (kN)	Ground water level from top of asphalt (mm)	Lateral position of wheel from the edge of the asphalt (mm).
Structure 22 (7.3 - 18.3.2002)			
0 – 480	20	500	0 – ±300 (at 50 mm intervals)
0 – 300	30 - 50	500	0, ±100, ±200, ±300
300 – 70000	50	500	0, ±100, ±200, ±300
Structure 21 (21.3 - 28.3.2002)			
0 – 480	20	500	0 – ±300 (at 50 mm intervals)
0 – 300	30 - 50	500	0, ±100, ±200, ±300
300 – 70060	70	500	0, ±100, ±200, ±300
Structure 23 (16.4 - 24.4.2002)			
0 – 480	20	1000	0 – ±300 (at 50 mm intervals)
0 – 300	30 - 50	1000	0, ±100, ±200, ±300
300 – 70000	70	1000	0, ±100, ±200, ±300

4.5 Earth pressure and deformation measurements

Earth pressure measurements monitored the earth pressure in the upper parts of the subgrade. Each structure contained a series of three earth pressure cells. All three cells functioned only in structure 22, in the other structures only two cells were functional. The results presented in Appendix 4 are averages of these measurements.

Vertical displacements and deformations in different layers of the structure were monitored. The drawings in Appendix 1 show the positions of the Emu-Coil sensors. Each structure contained six Emu-Coil pairs. The planned distance between the sensors in the middle of the subbase and base course in the beginning of the test was 200 mm. The planned distance between sensors elsewhere in the structure was 80 mm. The measuring accuracy of Emu-Coil sensors in the same layer with the same intervals varied between 0.5% - 19% relative error.

Resilient deformations on the surface of the structure were monitored with an accelerometer. Each structure had a measuring box, in which the accelerometer was placed during the loading. In addition, permanent deformations of the structures' surfaces were monitored by profilometer measurements. The results for all displacement measurements are presented in Appendix 5.

4.6 Bearing capacity and DOR measurements after testing

After the testing, changes in the bearing capacities of the structures were studied with both falling weight deflectometer and Loadman measurements. The quality of the asphalt was tested with DOR measurements conducted after the testing. The measurement results are presented in Appendix 6.

4.7 Distress surveys

Distress in the structures was monitored during the testing. The distress was photographed and recorded on a map. No large cracks were discovered in the structures, but some narrow longitudinal cracks were observed. Table 4.6 presents the formation of cracks in different structures.

Table 4.6. Formation of cracks in the structures.

Structure	N number of passes	Number of cracks	Cracks (length, cm)
21	27000	0	0
21	32100	3	60
21	52500	3	110
21	70060	4	140
23	40020	0	0
23	70000	1	100

5 DISCUSSION

5.1 Quality of construction

The starting point for designing the test structures was that the structure would be designed to correspond to the structure of low-volume roads. In the comparison of the quality of construction below, the values measured in the structure are compared with corresponding quality requirements laid down by the Finnish Road Administration Finnra TYLT /Tielaitos 1994/. However, these values were not aimed at, especially as regards bearing capacity. The values are presented in order to have an idea of the relation of the test structures to ordinary road structures.

The structure was constructed carefully to correspond to the quality of actual road building. The grain size distribution and the positions of the pavements fulfilled the requirements in TYLT. Because the construction site is small and the basin narrow, it was difficult to reach the same kind of quality during construction as for larger sites. This applies to the thickness and quality of the asphalt in particular. Figure 5.1 shows how the asphalt was clearly thicker than the planned 50 mm on test sections 22 and 23.

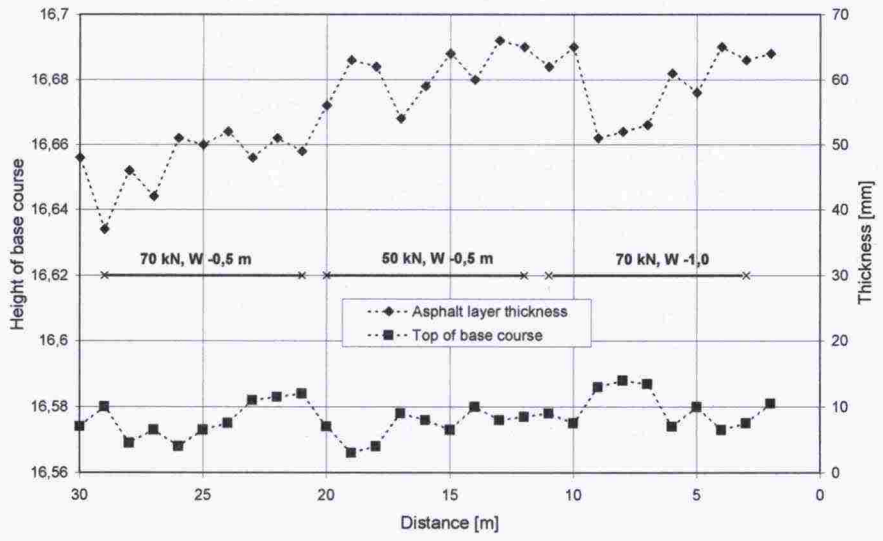

Figure 5.1. Asphalt thickness and moisture level of the top of the base course.

Density measurements were taken from the top of the subgrade after the layer was thawed. According to density measurements, the sand layer's average degree of compaction as measured by a sand cone volumeter and improved Proctor tests was 95.3% and the individual minimum value 93.2% (Appendix 2). Troxler density measurements on the subbase crushed gravel (Appendix 2) gave the average degree of compaction as 98.1% and the individual minimum value 97.1%. The Troxler measurements conducted cannot be considered completely reliable, rather, they give a general idea. The base course's degree of compaction was defined from the ratio between sand

cone volumeter test and improved Proctor test results. The average degree of compaction was 96.4% and the lowest value 95.0%. The degrees of compaction for all layers clearly meet the requirements set out in TYLT.

E_2 determined by a falling weight deflectometer (FWD) on the centre line of loading was 96 MPa. The best average results were achieved on the middle structure, structure 22. The FWD-determined value for the base course varies between 99 and 108 MPa, the average being 103 MPa. According to TYLT, the bearing capacity minimum value E_2 determined by a falling weight deflectometer for subbase is 105 MPa and for base course 215 MPa. Thus, TYLT requirements were not met as regards bearing capacity.

The bearing capacity of the whole structure was measured from the top of the asphalt using FWD measurements. The measurements were conducted for both ground water levels. The temperature-corrected bearing capacity values E_2 for the higher ground water level varied between 103 and 165 MPa and for the lower level between 136 and 189 MPa. These measurements also showed that the bearing capacity of structure 21 was the weakest and the bearing capacity of the middle structure was the highest.

The thickness of the asphalt was calculated from the levelling results and determined by eddy-current measurements (Appendix 2). According to the measurement results, the asphalt of the middle structure (structure 22) was clearly the thickest (60.8 mm). The average thickness on structure 23 was 59 mm and that of structure 21 50 mm. The differences were large and probably due to the fact that it was difficult to correctly adjust the asphalt paver on such a short structure.

The density of the asphalt was measured with DOR measurements after testing (Appendix 6 and Figure 5.2). According to the results, the density varied between 2.25 and 2.37 kg/dm^3, the average being 2.3 kg/dm^3. The measurements showed that the asphalt was not uniform in quality.

The bearing capacity of the structure was also measured after the testing ended. The bearing capacities calculated at that time varied between 142 and 237 kPa. These measurements showed that the middle structure (structure 22) had the highest bearing capacity (on average 217 kPa) and structure 23 was the weakest (on average 196 kPa). Presumably the structure compacted during the testing, because according to FWD measurements, the bearing capacities increased in the testing. Figure 5.2 presents the densities of the asphalt and the results of FWD measurements made from the top of the asphalt.

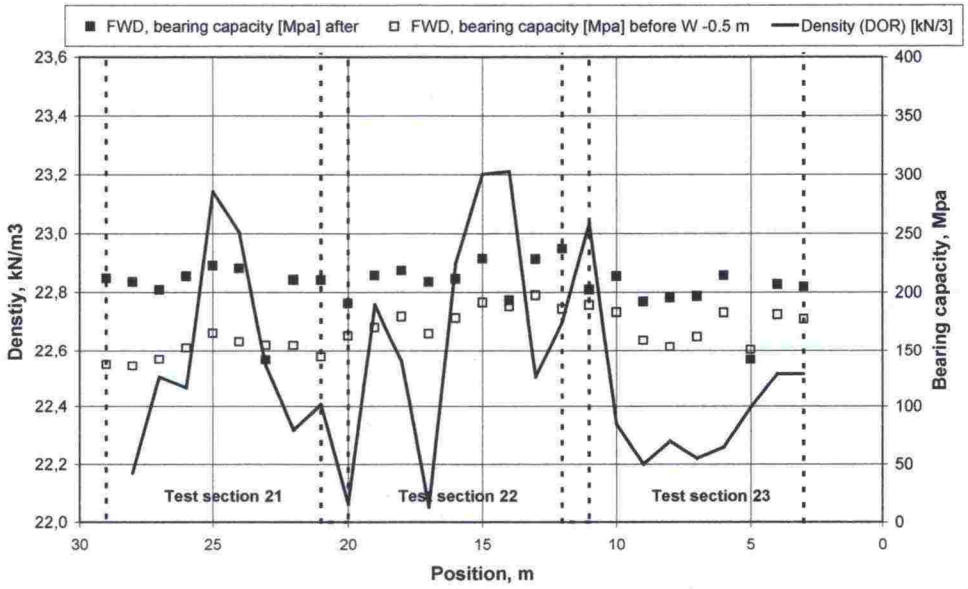

Figure 5.2. The bearing capacities of different test sections according to falling weight deflectometer measurements before and after the loading test, and asphalt densities according to DOR measurements.

5.2 Rutting speeds of the structures

The rutting of the structures' surfaces was monitored with profilometer measurements. Three cross sections were monitored in each structure, and the average rutting speed was calculated from their averages. Because the thickness of the asphalt was not identical in all the structures, the calculations converted the deformations of the thicker structures (22 and 23) layer by layer in relation to the thickness of the asphalt to correspond to deformations in the structure with the target thickness (50 mm). The overall estimate was that the rut depth of structures over 60 mm thick asphalt with the ground water at the higher level was increased by 14.5%. If the ground water level was lower, but the thickness of the asphalt was over 60 mm, rut depth was increased by 10%.

In addition, the rutting of a structure with a load of 50 kN in moist conditions was estimated by calculation. This estimate was based on the rutting speed with 50 kN load obtained at the beginning of the test. Figure 5.3 shows the rutting of different structures defined in this way as a function of the number of passes.

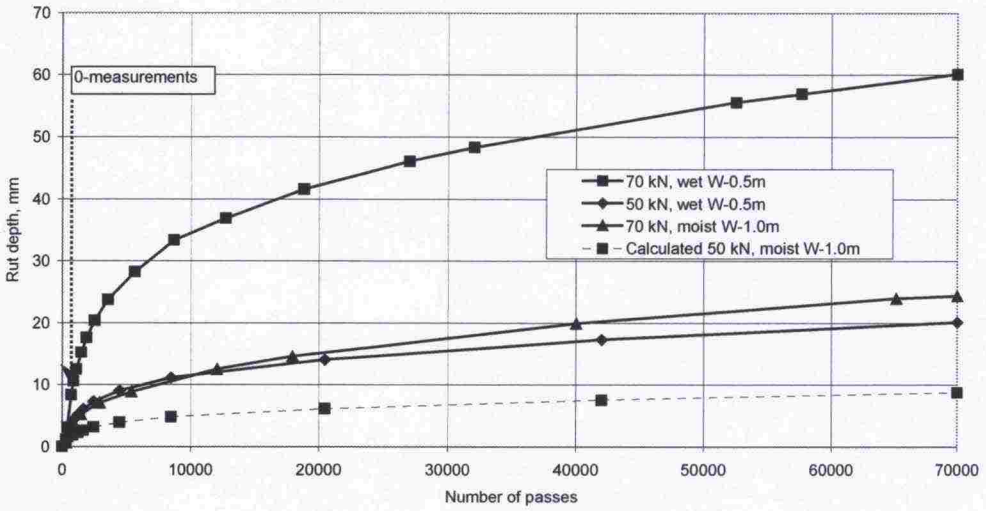

Figure 5.3. The rutting of different structures in relation to the number of passes.

The rut depth estimated by calculation for 50 kN load in moist conditions is 8.8 mm when the number of passes is 70,000. After making the correction for the thickness of the asphalt, the estimated rut depth for 70 kN load is 24.4 mm. Correspondingly, with the higher ground water level, the rut depths are 20 mm and 60 mm. That is, rut depth is 2.8 to 3 times higher when the load is increased from 50 kN to 70 kN. Raising the ground water level by 0.5 metres increases rutting 2.2 to 2.45 times. If both load and ground water level increase, the rutting increases 6.8 times. These ratios are only approximate and naturally depend on the structure, its state of compaction etc.

5.3 Distribution of permanent deformations in the structure

Permanent deformations in the structure were monitored with Emu-Coil, settlement profile and eddy-current measurements. Settlement profile and eddy-current measurements were only conducted at the beginning and end of the whole testing. The rutting of the asphalts' surface was monitored with profilometer measurements. Figure 5.4 presents the share of displacement in different layers in the total rutting combined from different measurements.

The graphs in Figure 5.4 follow the same pattern surprisingly well. The largest share of rutting (47 to 59%) for each load occurs in the subgrade. When the ground water was lower, a greater share of displacements occurs higher up in the base course. When the ground water level is raised, a proportionally larger share of settlement occurs lower down in the gravel and sand. The share of the asphalt of the rutting was 3.5 to 6% that of the crushed rock in the base course 15 to 23% and crushed gravel in the subbase 23 to 27%.

The permanent deformations in different layers at the end of testing are shown in Figure 5.5. The calculation of permanent deformations takes into account the thickness of the layers, the distances between the Emu-Coil

sensors and the average values from Emu-Coil sensors at the same depth in the base course. The thickness of the subgrade is assumed to be the total distance to the bottom of the basin.

The same phenomena can be observed in Figures 5.4 and 5.5: a significant share of permanent deformations occur in the subgrade and the concentration of a relatively larger share of deformations in the lower layers when the ground water level is higher. The development of permanent deformations as the number of passes increases in structure 21 is presented in Figure 5.6.

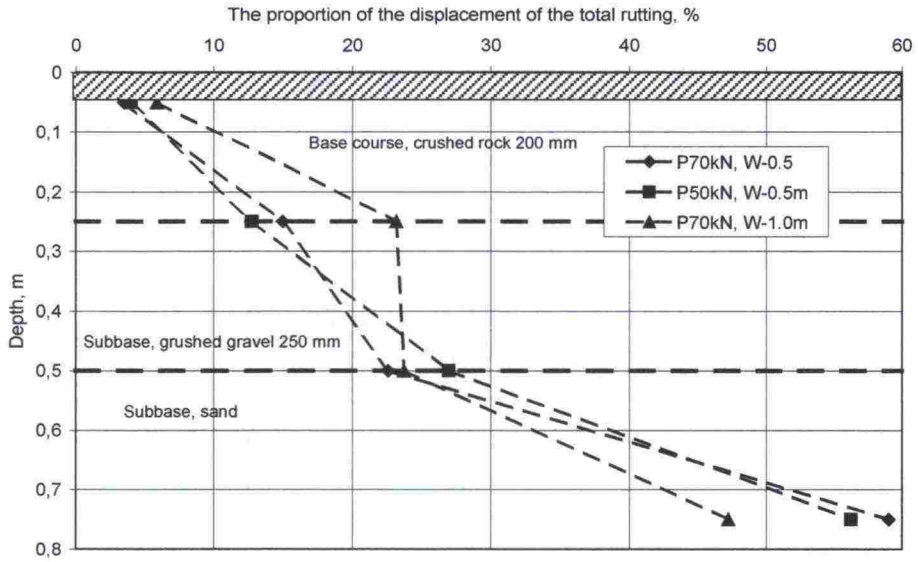

Figure 5.4. The share of deformations in different layers of the total rutting.

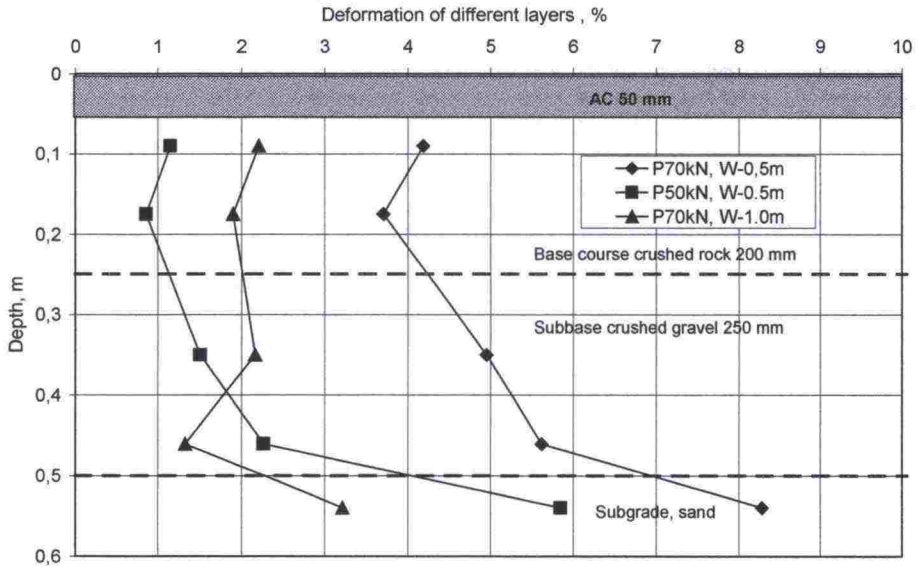

Figure 5.5. The relative permanent deformations in the different layers.

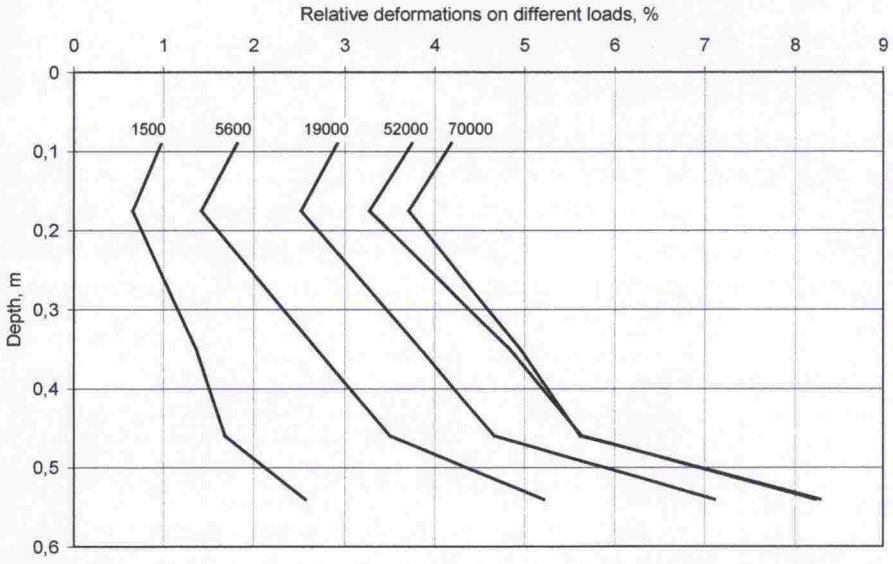

Figure 5.6. Structure 21. The development of permanent relative deformations as the number of load repetitions increases.

Figure 5.6 shows that the deformations first concentrate, to a certain extent, in the upper part of the structure. As the upper part becomes compacted, the development of deformations focuses on the lower layers.

5.4 Fourth power rule

The fourth power rule is used for estimating the damage to the asphalt of a road. The rule is empirical and was developed on the basis of AASHO road test conducted in the United States in the 1950s /AASTHO 1962/. The tests monitored different road structures and their distress over a period of many years. The monitored sites could mostly be classified as high-volume roads and their bound layers were thick, that is, they were not low-volume roads. The rule says that the ratio of distress or the number of load repetitions increases in relation to loads according to Formula 5.1, when the tyre pressure used in the loading remains the same. When estimating the rutting of roads with an asphalt surface layer, the index n value used, on the basis of AASHO road tests, is usually 4.

$$E = \left(\frac{P_x}{P_{st}} \right)^n \qquad (5.1)$$

in which

E		equivalent coefficient of the load
P_x		the axle load studied
n		index
P_{st}		standard axle load

Figure 5.7 presents the ratio of the number of passes for different rut depths determined for 50 and 70 kN loads on a wet structure (the ground water level at –0.5 m from the top of the asphalt). Because no significant distress besides rutting was observed in the structures, the distress was only described as rut depth. The share of compaction (the first 900 passes) has been excluded from calculating the ratio of the number of passes. The calculations took into account the variation in the thickness of the asphalt in different structures. The asphalt thickness used was the original design's target thickness, 50 mm. In addition, it was necessary to linearly extrapolate the rutting curve for the 50 kN load for rut depths of over 18 mm (Figure 5.7 calculated values).

According to Formula 5.1, the development of distress should be independent of rut depth. The value for the equivalent coefficient for the standard load 50 kN and the axle load studied 70 kN is approximately 3.8 (the horizontal line in Figure 5.7) when the value used for the index n is 4.

AASHO test: $(P_s/P)^n = (70\ kN / 50\ kN)^4 = 3.8$

However, the ratios of number of passes (N/N_s) calculated from rut depths are clearly larger, in the order of 6 to 18. The back calculated index n in Formula 5.1 varies between 5.5 and 8.5. Thus, the results reveal that the fourth power rule is not valid for low-volume roads. The HVS tests in the low-volume road project indicated the same.

HVS Spring – overload: $(N/N_s) = 6 - 18 = (70\ kN/50\ kN)^n \Rightarrow n = 5.5 - 8.5$

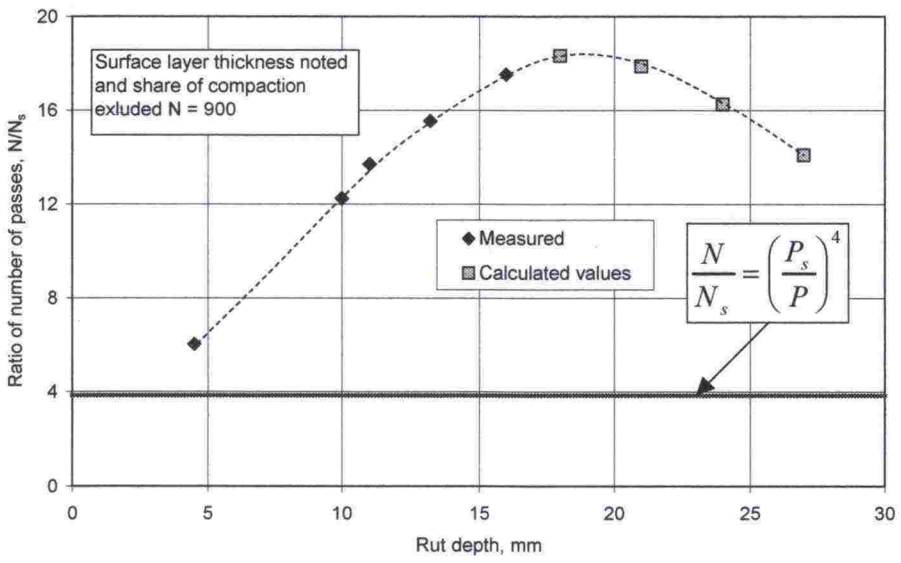

Figure 5.7. Ratio of number of passes with different rut depths. The figure shows the coefficient for the number of 50 kN load repetitions needed to achieve the same rut depth as for the 70 KN load in the same conditions. For rut depths of over 18 mm, it was necessary to extrapolate the rut depth for the 50 kN load (calculated values). $(N/N_s) = (P_s/P)^n$

The tests also aimed at using the fourth power rule to discover the volume of traffic after which road distress is not governed by fatigue but permanent deformations in lower layers. It is assumed that fatigue governs distress on small rut depths when the fourth power rule applies. Figure 5.7 shows that when rut depth is less than 2 to 2.5 mm, the fourth power rule probably applies. This rut depth corresponds to approximately 200 to 400 passes. On the basis of this, it can be said that with traffic volumes greater than 200 to 400 passes, permanent deformations in the structure begin to govern road design.

The fourth power rule is an empirical relationship that is established on the basis of a statistical analysis, and the only factor taken into account is load. Especially in cases in which behaviour is governed by permanent deformations, quite non-linear in nature, it is not surprising that the fourth power rule does not work. Thus, such a simplified rule cannot be used for modelling the road deformations on low-volume roads.

5.5 Relations of deformations

The relation of resilient and permanent vertical deformations in different materials was compared by Emu-Coil measurements. Resilient deformation is the total deformation caused by one pass, which includes both permanent and dynamic deformation. The share of permanent deformation of the resilient total deformation is, however, so small as to be trivial. Figure 5.8 presents these relations of deformations for subgrade sand. The results clearly show a threshold value for resilient deformations / stress state, after which permanent deformations clearly increase faster. Similar behaviour could be observed in other materials, although the results varied more. The phenomenon is familiar from geotechnics, in which the limit is described, for instance, as exceeding the soil elasticity. The limit deformation presented in Figure 5.8 commonly depends not only on the material, but also its state (moisture, density and stress state).

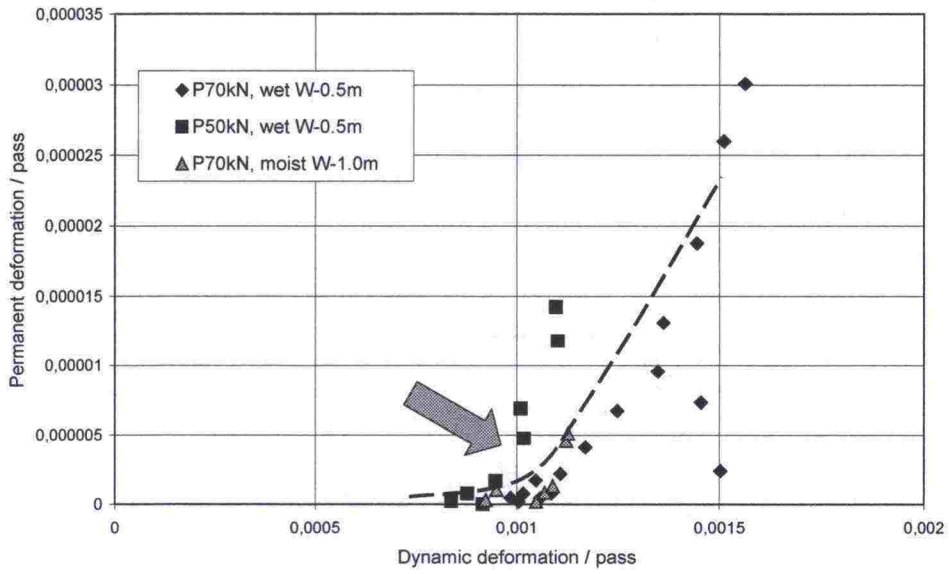

Figure 5.8. The relation of dynamic and permanent deformations in subgrade sand.

5.6 Changes in bearing capacity on the basis of falling weight deflectometer results

The bearing capacities measured from the tops of the different pavements during construction were of the same order, and the normal increase in bearing capacity by layers did not occur, except between the asphalt and the base course. This suggests that the structure constructed in winter and compacted when dry did not compact as desired during construction. It did not compact until during loading. This happened despite the target degrees of compaction determined by the sand cone volumeter being achieved during construction. The relatively light compaction during the construction was intended to represent a structure loosened by frost. Water was then later added to represent the increase in the water content during the thawing.

The bearing capacities measured by falling weight deflectometer increased during the test in all structures. The greatest increase occurred in the structure that was, in advance, the weakest and most loaded, structure 21, in which the bearing capacity increased from 161 Mpa to 206 MPa (45 MPa). In structure 22, the bearing capacity increased 20 MPa and in structure 23, 12 MPa. That is, all the structures compacted during the test, even structure 21, which rutted significantly. Only a few cracks were observed in structures 21 and 23 after the test. Thus, it can be assumed that the structures did not significantly crack from the bottom of the asphalt, where cracks usually begin.

5.7 Cross directional rutting

The cross directional rutting of the pavement was monitored on the basis of laser profilometer results. Figure 5.9 shows changes in the cross sections measured from the centre of structure 21 in relation to the number of passes. The figures show the limits of the loading area, that is, the points that the outer wheel of the dual wheel reached during loading.

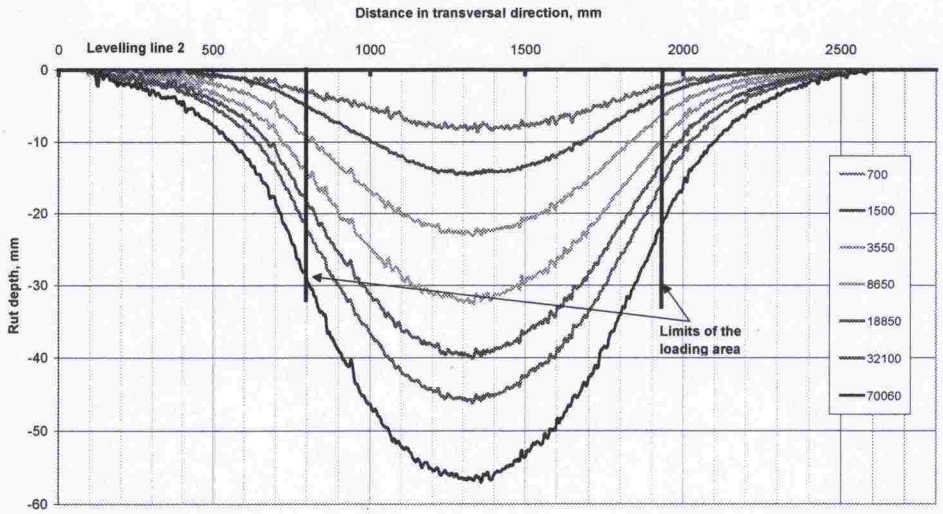

Figure 5.9. Structure 21. Cross directional rutting of the structure.

The width of the rutted area was the greatest in structure 21, in which the rut depth was also the greatest. The formation of a upheaval outside the loading area was not much observed in the tests. This is probably due to two factors: the majority of rutting occurred deep in the structure and was, by nature, more volumetric strain (compaction) than deviatoric strain.

Cross directional rutting of the pavements was monitored with settlement profile measurements. Figure 5.10 shows the rutting of pavements in the most rutted structure, structure 21. The figure shows that rutting in all pavements seems to be mostly compaction and there is no significant shearing action. When estimating the distribution of the rutting area in the pavements from the figure, it can be seen that deeper down in the structure, the rutting spreads over a very wide area.

In the depth of 0.5 metres, on top of the sand layer, the width of the rutted area was approximately 2.5 metres, while the width of the entire loading area on top of the asphalt was 1.15 metres. This means that the load spreads in the sand layer according to the ratio 1:1.35. The width of the rutted area reveals over how wide an area stresses were distributed in the layer. A commonly used assumption in geotechnical engineering is that the stresses are distributed in a ratio 2 : 1 to the soil layers beneath. Thus, in road structures the stresses are clearly distributed over a wider area than the above assumption would predict, causing displacements to also de-

crease. In other layers, the distribution is even wider in relation to the thickness of the layers above, the ratios being approximately:

- bottom of the asphalt / top of base course 1 : 4.5
- top part of base course (100 mm) 1 : 2.7
- bottom part of base course / top of subbase 1 : 1.7
- bottom of subbase / top of subgrade 1 : 1.35

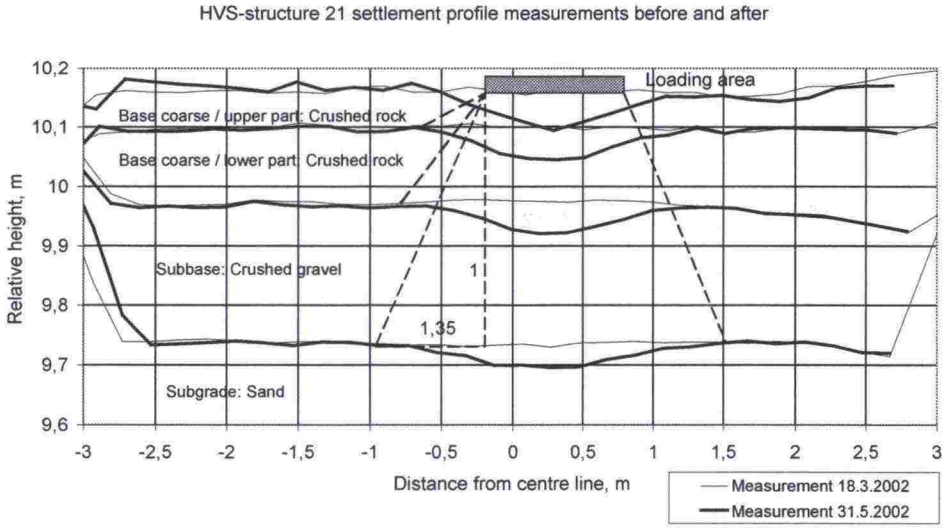

Figure 5.10. The rutting of pavements in structure 21 according to settlement profile measurements.

5.8 Changes in water content in the layers with different ground water levels

Changes in the water content of the pavements was monitored with radiometric measurements before and after testing. Measurements were taken with the ground water level at the highest level, –0.5 m from the top of the asphalt and deeper down, at –1.0 metres. Measurements were also conducted once approximately two months after the test ended, at which time the water level had receded lower. There was a leak in the rock basin, above the level of which (about -1.5 metres) the water table level did not reach after the test.

The averages of different radiometric measurements for ground water levels, –0.5 m, –1.0 m and >–1,0 m, are calculated in Figure 5.11. The highest radiometric measurements (to approximately 300 mm) are generally not reliable. According to the measurement results, the water content does not significantly change although the ground water level changes. On the other hand, although according to measurements changes in the water content are small, it has a significant effect on permanent deformations. This is especially true in the crushed gravel of the subbase (change 0.3%) and the top parts of the sand layer (change 0.3%). The degree of saturation in the top

part of the sand layer with the lower ground water level is, on the average, over 90%. The capillary rise of sand according to grain size distribution can be estimated at 400 mm. Average water contents, their changes and the relative proportions of the changes in different layers are presented in Table 5.1.

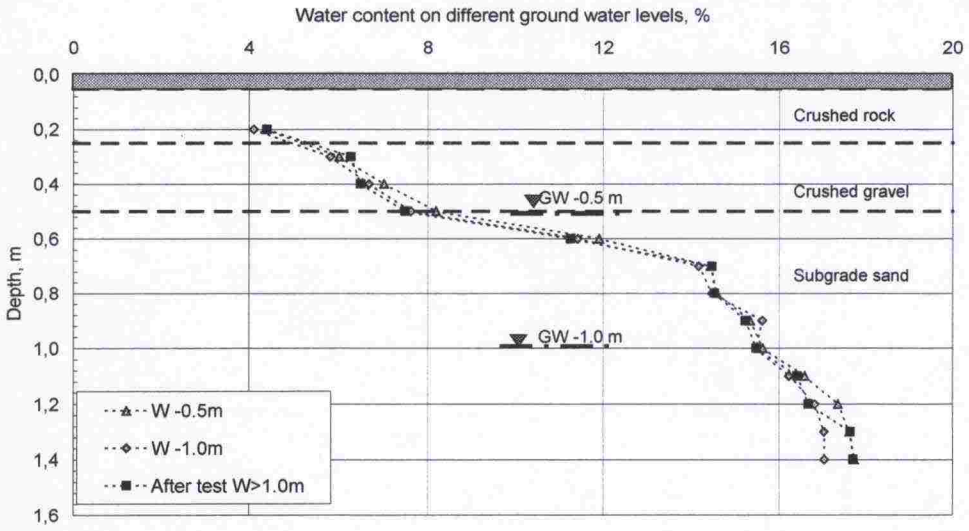

Figure 5.11. Water content at different ground water levels.

Table 5.1. Water content, its average change and relative proportion in different layers when ground water is raised from –1.0 m to –0.5 m.

Material	Crushed rock	Crushed gravel	Sand top 500 mm	Sand, lowest part
Average water content %	1.9	3.6	10.2	13.1
Average change %	0.18	0.27	0.28	0.63
Proportion %	9.5	7.7	2.7	4.8

Although the reliability of radiometric measurements as absolute values with such small changes is not high (the change in water content also depends on the change in dry bulk density), the measurements show how even small changes can have a dramatic effect on the generation of permanent deformations. The primary reason behind this phenomenon is probably the fact that as the relative amount of water increases, the thickness of the moisture film surrounding the solid matter increases (the number of water molecule layers increases), and the strength of the electronic bond decreases. The force in question is called matric suction, which is also known to depend on the mineralogical characteristics of the material.

5.9 Back-calculated resilient moduli for the sand layer

The earth pressure in the structure was only monitored with earth pressure cells in the sand layer. The functioning of earth pressure cells in other pavements was assumed to be so inaccurate that they were not instrumented. The resilient modulus for the layer was calculated according to Formula 5.2 as the ratio of the change in the transient stress state caused by one loading (earth pressure σ_{zmax}) and the change in transient elastic displacement ε_{zmax} (Emu-Coil):

$$E = \frac{\Delta\sigma_{z\max}}{\Delta\varepsilon_{z\max}}. \qquad (5.2)$$

in which E dynamic resilient modulus (MPa)
$\Delta\varepsilon_{zmax}$ resilient, elastic deformation in vertical direction
$\Delta\sigma_{zmax}$ transient vertical earth pressure change

Figure 5.12 shows the sand layer resilient moduli in different structures and the results from Loadman bearing capacity measurements of the gravel layer during construction. The averages for the moduli on different loading levels on the basis of measurements and laboratory tests are presented in Table 5.2.

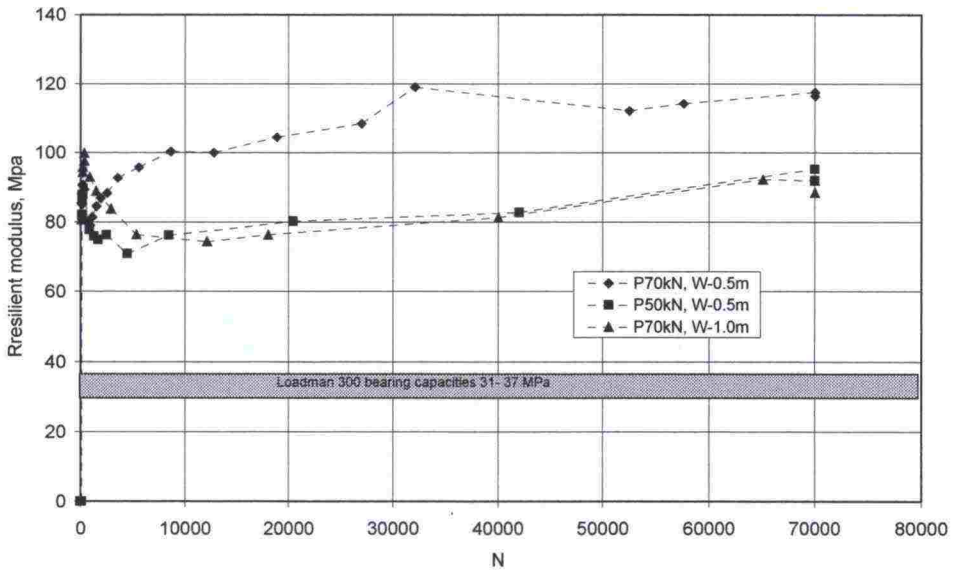

Figure 5.12 The back-calculated resilient moduli of different structures.

Table 5.2. Resilient modulus averages (MPa) in different structures on different loading levels.

Loading .. level, kN	Laboratory tests (MPa)	P70kN, W-0.5m; MPa	P50kN, W-0.5m; MPa	P70kN, W-1.0m; MPa
50	106 - 117	90.4	84.3 / 80.9 (total loading)	94.5 / 94.8
70	127 - 139	98.3	-	80.5 / 86.9

The measured resilient modulus can be considered the real modulus of the structure's operational condition and it should correspond to the resilient modulus value. Contrary to expectations, the resilient modulus was the smallest in the case when the ground water level was lowest and load greatest. Therefore, Table 5.2 presents the average from two measurements and the value calculated from the greater stress state. It can be assumed that the earth pressure cells functioned unreliably in this structure. As for other results, the moduli behaved largely according to expectations. Laboratory results give clearly larger resilient modulus values than the test results. This is largely due to the fact that the laboratory tests were conducted at a water content of 8%, while the water content realised in the structure was clearly higher, in the order of 14%. The increase in the resilient modulus of the operational condition is probably mostly a consequence of compaction of the material during loading.

6 CONCLUSIONS

A great deal of measurement data was generated in different phases of the HVS tests. In this report, the data has been analysed in view of the aims of the study. The results will be analysed further in future studies. Further research will look more deeply into the ways permanent deformations are created and the effect changes in water content have on them.

On the basis of research already carried out, it can be concluded that:

- It is difficult to achieve target quality in constructing a small test site, in particular as regards the thickness of the asphalt.
- The deformations in the structures were compaction in nature. No significant generation of upheavals occurred next to the ruts, and the bearing capacities of the structures increased during the tests. Only very few cracks were observed in the structures towards the end of testing.
- Rut depths increased 2.8 to 3 times when the axle load increased from 50 kN to 70 kN. Correspondingly, rut depths increased 2.2 to 2.5 times when the ground water level rose 500 mm.
- The majority of permanent deformations in all structures occurred in the subgrade sand (47 to 59%).
- When the ground water was at the top of the subgrade (-0,5 m from the asphalt) a relatively larger share of permanent deformations occurred in the subbase gravel and the subgrade. When the ground water was lower (–1.0 m) a greater share of displacements occurred higher up in the base course.
- The fourth power rule does not apply to low-volume roads. It can be estimated on the basis of the rule that on loading levels 50 to 70 kN and traffic volumes greater than 200 to 400 passes, the design is governed by permanent deformations in the structure, not fatigue.
- Permanent deformations in the materials showed a clear increase after a threshold value corresponding to a certain stress state was exceeded.
- The width of the rutted area also depends on rut depth. When the ruts are deepest, the rutted area also is widest. In practice, drivers' behaviour when driving on a rutted road also affects the situation.
- Stresses in the road's pavements spread to a relatively wide area even with thin asphalt, thus also decreasing displacements.
- According to radiometric measurements, the water content of the pavements increased approximately 0.2 to 0.5 % units when the ground water level was raised to the top of the subgrade.
- The back-calculated resilient moduli for the sand layer gave results 15 to 40% lower than the values determined in the laboratory. Contrary to expectations, the back-calculated resilient modulus was the smallest in the case when the load was the greatest and ground water level lower.

7 LITERATURE

AASHTO. The Aasho Road test. Report 7 Summary Report. Highway Research Board. Special report 61G. 1962.

Chen J-S. ja Lin K-Y. Evaluation of an Accelerated Pavement Testing Facility and development of its Load Equivalence Factors. Journal of Testing and Evaluation.Vol. 30 No 2. March 2002. pp. 103-109.

Ehrola E., Liikenneväylien rakennesuunnittelun perusteet. Rakennustieto. 1996. Helsinki. s. 357.

FHWA. 2002. U.S. Department of Transportation. Comprehensive truck size and weight study. TS&W Final Report. Vol 3. Appendix. FHWA homepage. www.fhra.dot.gov.reports/tswstudy/TSWfinal.htm

Kivikoski H. & Laaksonen R., 2002, Deformaation mittausmenetelmät. Työraportti. VTT Rakennus- ja yhdyskuntatekniikka.

Kolisoja P., 1996. Sitomattomien materiaalien moduulit, Vuoden 1995 kokeet. Tielaitoksen selvityksiä 34/1996. Helsinki 1996.

Laaksonen R. & al., 1999. ICT -moduuli. VTT Yhdyskuntatekniikka. Espoo 1999.

Tielaitos, 1985, Normaalimääräykset ja ohjeet, Mitoituskansio Osa B

Törnqvist J. & Jauhiainen P., 2001, ICT-koe tien rakennekerrosmateriaalien deformaatioherkkyyden määrittämisessä, Tiehallinnon selvityksiä 63/2001, Tiehallinto, s. 47.

Wiman L.G. Accelerated load testing of pavements, HVS-Nordic tests in Sweden 1999. VTI rapport 477A-2001. Linköping. p. 93.

8 APPENDICES

APPENDIX 1Instrumentation and detail drawings
APPENDIX 2Measurements during construction
APPENDIX 3Laboratory results
APPENDIX 4Earth pressure measurements
APPENDIX 5Deformation measurements
APPENDIX 6Measurements after testing

APPENDIX 1. INSTRUMENTATION AND DETAIL DRAWINGS

Test sections

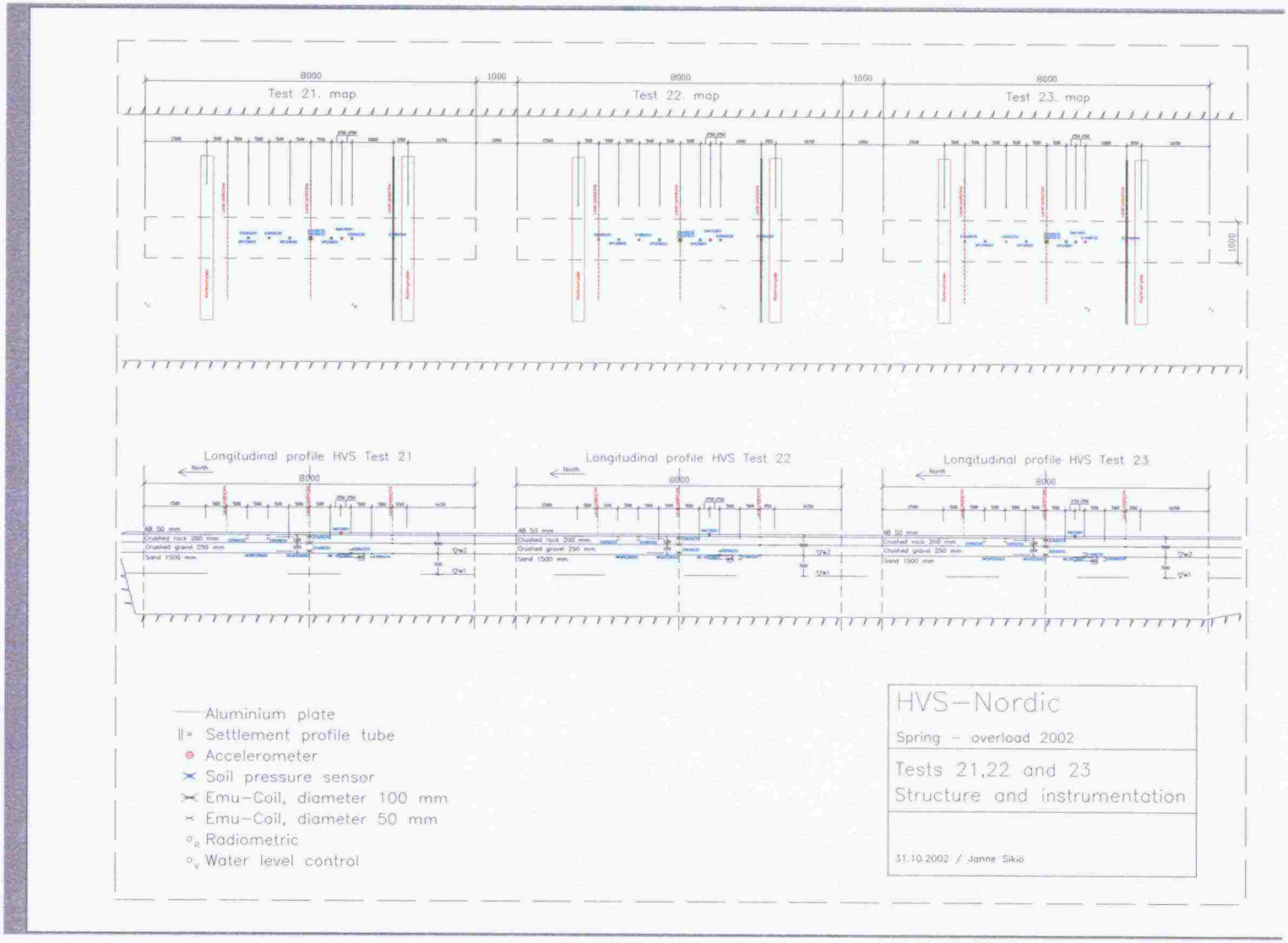

Test structure 21

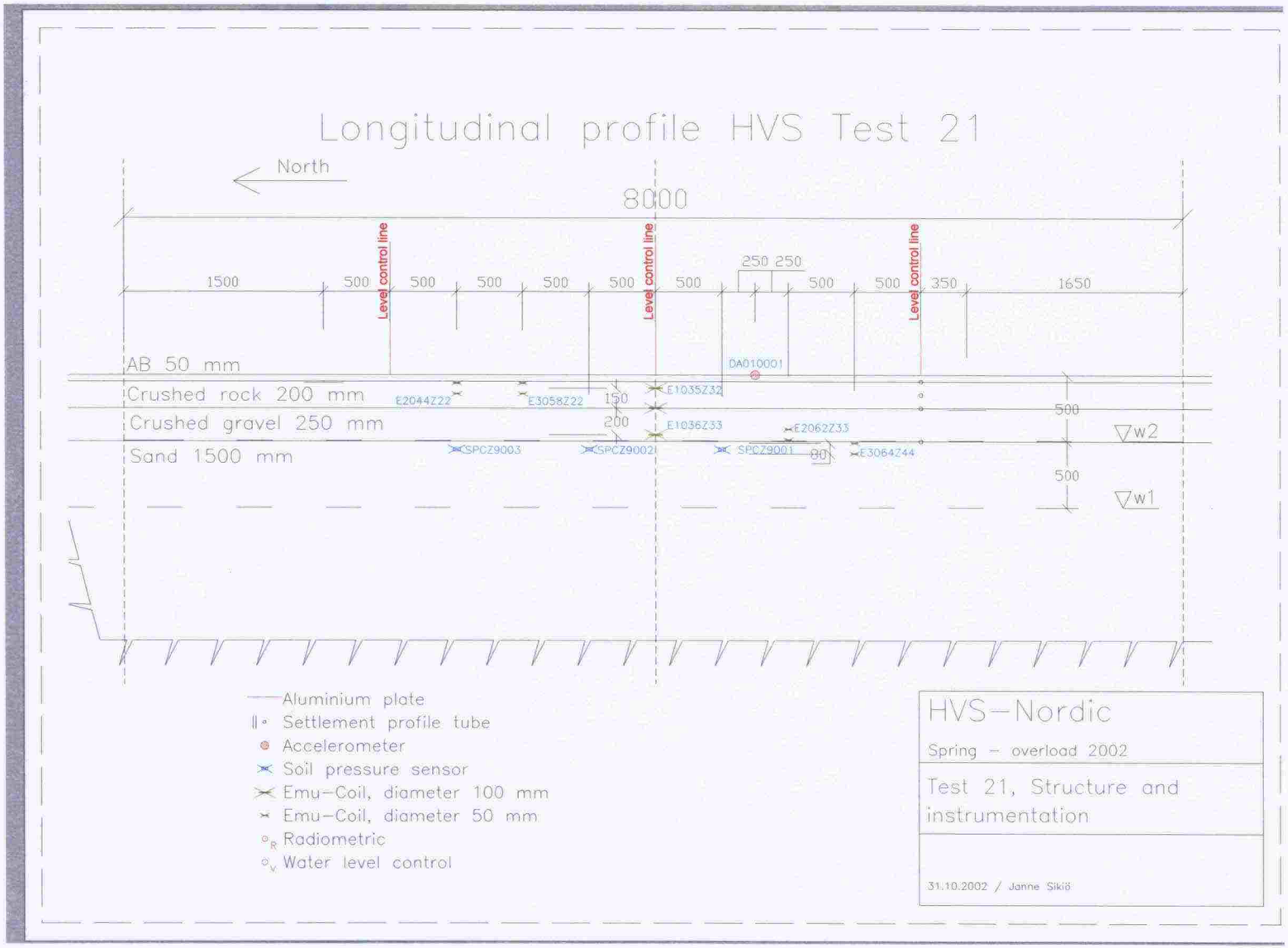

Test structure 22

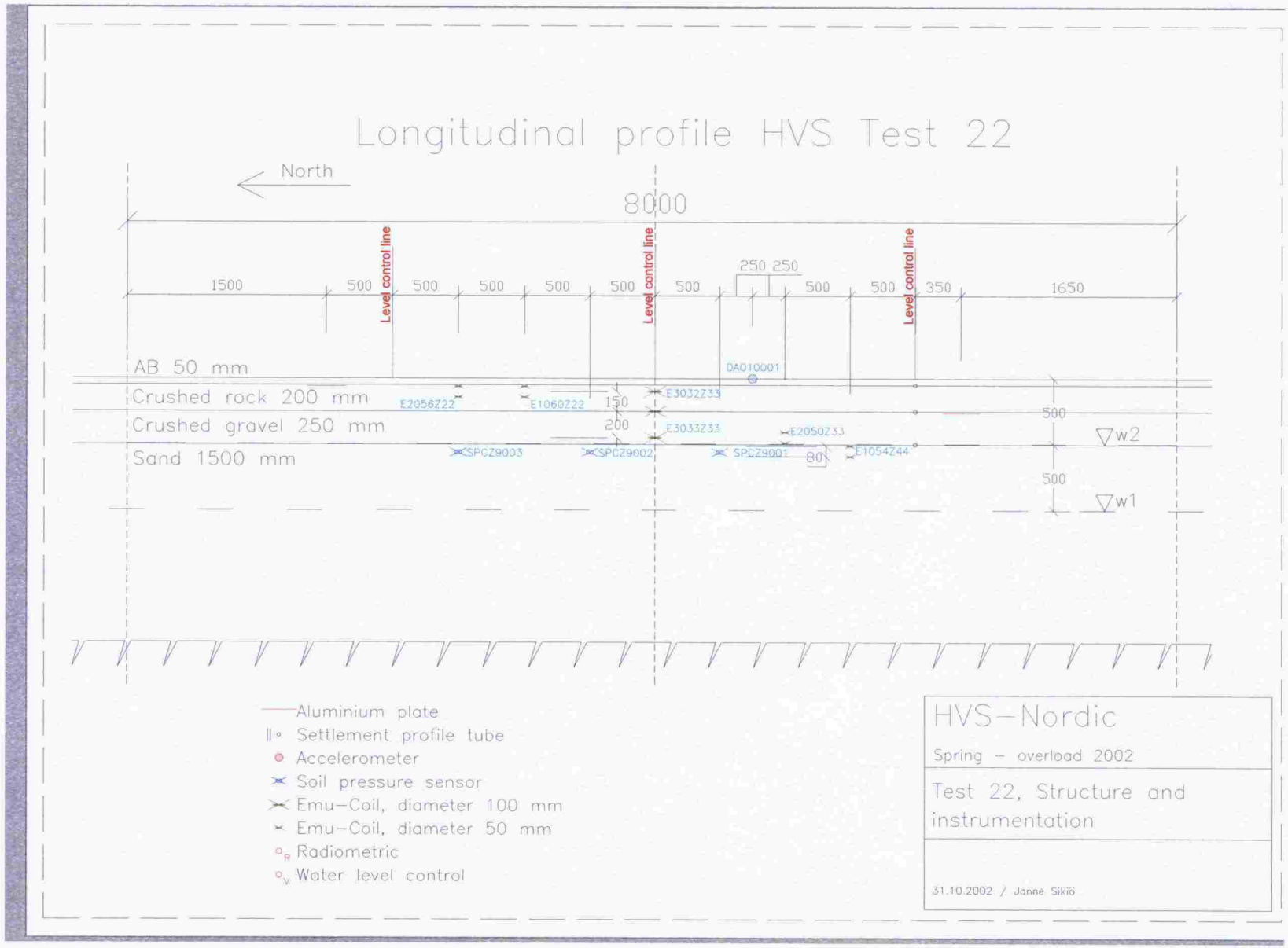

Test structure 23

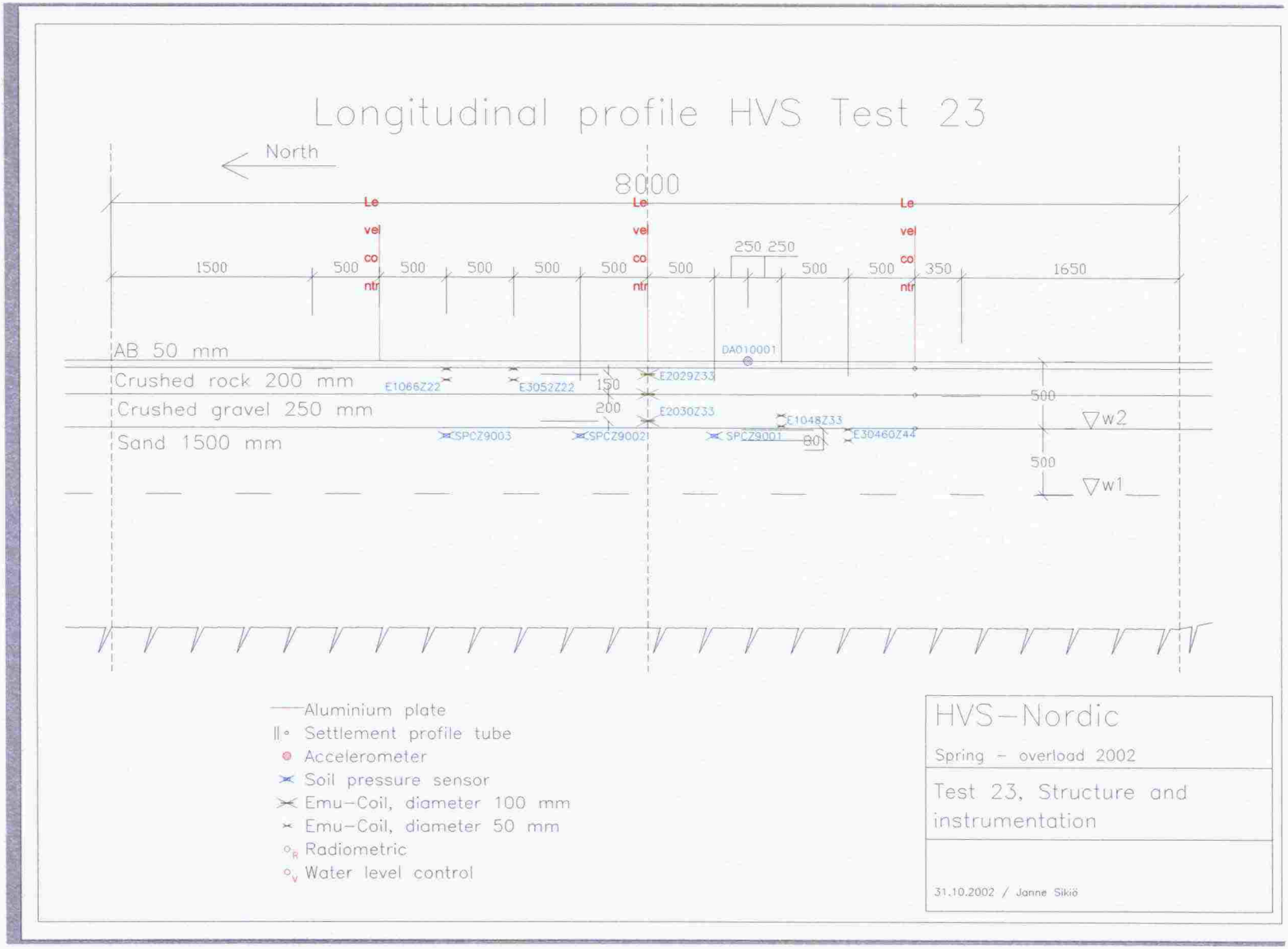

Cross section and instrumentation of the structure

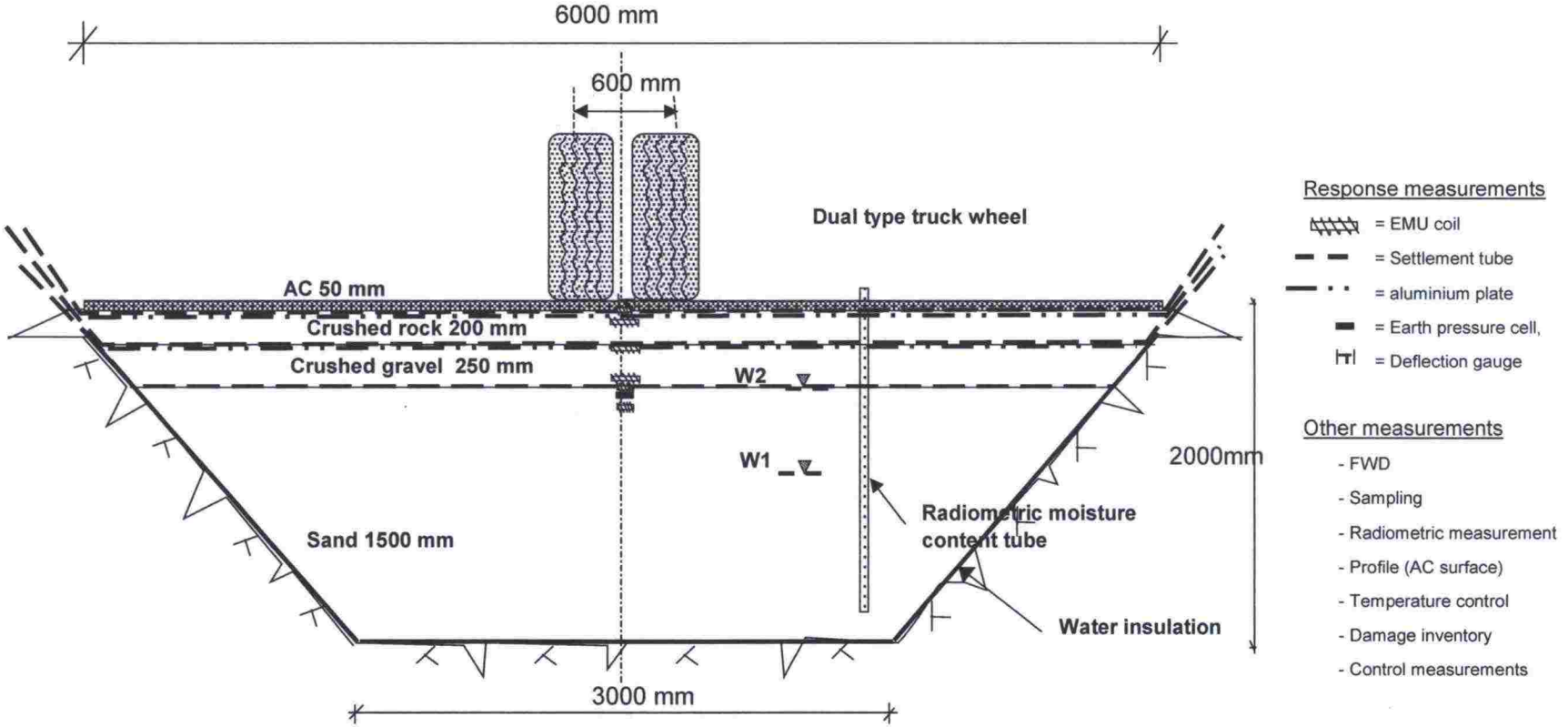

APPENDIX 2. QUALITY CONTROL AND BEARING CAPACITY MEASUREMENTS DURING CONSTRUCTION.

Average thickness of layers by levelling and eddy-current measurements.

Structure 21, 70 kN W –0.5 m

Layer	Average thickness, mm	Variation,	Eddy-measuremen	Variation,
Surface layer 50	50.1	2.1	47.7	2.1
Base course crushed 200 mm	199.6	6.9		
Subbase crushed 250 mm	235.7	12.6		

Structure 22, 50 kN W –0.5 m

Layer	Average thickness, mm	Variation,	Eddy-measuremen	Variation,
Surface layer 50	60.8	4.8	62.6	0.7
Base course crushed 200 mm	178.1	7.1		
Subbase crushed 250 mm	246.0	9.6		

Structure 23, 70 kN W –1.0 m

Layer	Average thickness, mm	Variation,	Eddy-measuremen	Variation,
Surface layer 50	59.0	7.1	57.5	1.3
Base course crushed 200 mm	183.4	9.5		
Subbase crushed 250 mm	252.8	11.5		

Density measurements of pavements

Troxler and sand cone volumeter results for sand. The maximum dry bulk density according to laboratory tests is 18.8 kN/m^3. The comparison of degree of density was carried out between that and the volumeter tests considered more reliable.

Measurement 23.1.2002	Water content w-% Troxler / sand cone volumeter	Bulk density, kN/m^3 Troxler / volumeter	Dry bulk density, kN/m^3 Troxler / volumeter	Degree of density %, volumeter / improved Proctor
Str 21	8.1 / 8.3	18.69 / 18.98	17.29 / 17.53	93.2
Str 22	6.2 / 6.5	18.69 / 18.93	17.60 / 17.78	94.5
Str 23	8.1 / 8.7	19.37 / 20.07	17.92 / 18.46	98.2
Averages	7.5 / 7.8	18.9 / 19.3	17.6 /17.9	95.3

Troxler results for crushed gravel. The maximum dry bulk density according to laboratory tests is 22.0 kN/m^3. The comparison of degree of density was carried out between that and Troxler measurements.

Measurement 1.2.2002	Water content w-% Troxler	Bulk density, kN/m^3 Troxler	Dry bulk density, kN/m^3 Troxler	Degree of density %, Troxler/ improved Proctor
Str 21	3.3	22.07	21.36	97.1
Str 22	3.4	22.42	21.68	98.6
Str 23	2.8	22.29	21.68	98.6
Averages	3.2	22.3	21.6	98.1

Troxler and sand cone volumeter results for crushed rock. The maximum dry bulk density according to laboratory tests is 18.8 kN/m^3. The comparison of density was carried out between that and the volumeter tests considered more reliable.

Measurement 8.2.2002	Water content w-% Troxler / sand cone volumeter	Bulk density, kN/m^3 Troxler / volumeter	Dry bulk density, kN/m^3 Troxler / volumeter	Degree of density %, volumeter / improved Proctor
Str 21	3.7 / 3.2	21.41 / 22.4	20.63 / 21.75	95.6
Str 22	4.0 / 3.4	21.45 / 22.40	20.60 / 21.60	98.5
Str 23	4.6 / 5.1	21.34 / 21.95	20.41 / 20.89	95.0
Averages	4.1 / 3.9	22.4 / 22.3	20.5 / 21.4	96.4

Bearing capacity measurements.

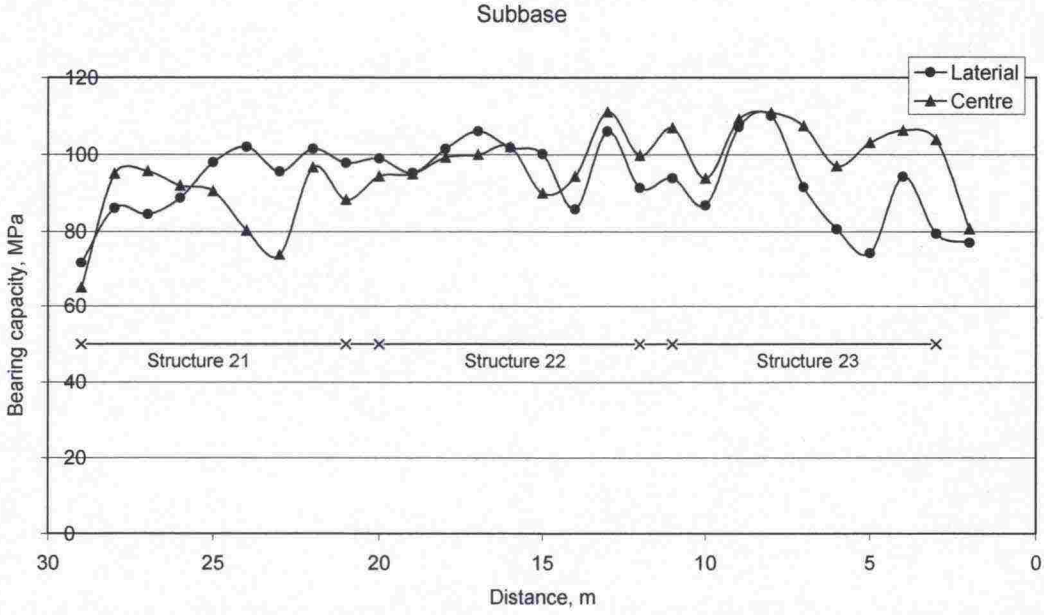

Falling weight deflectometer measurements Bearing capacity of the crushed gravel layer. Lateral line 800 mm right of the centre line.

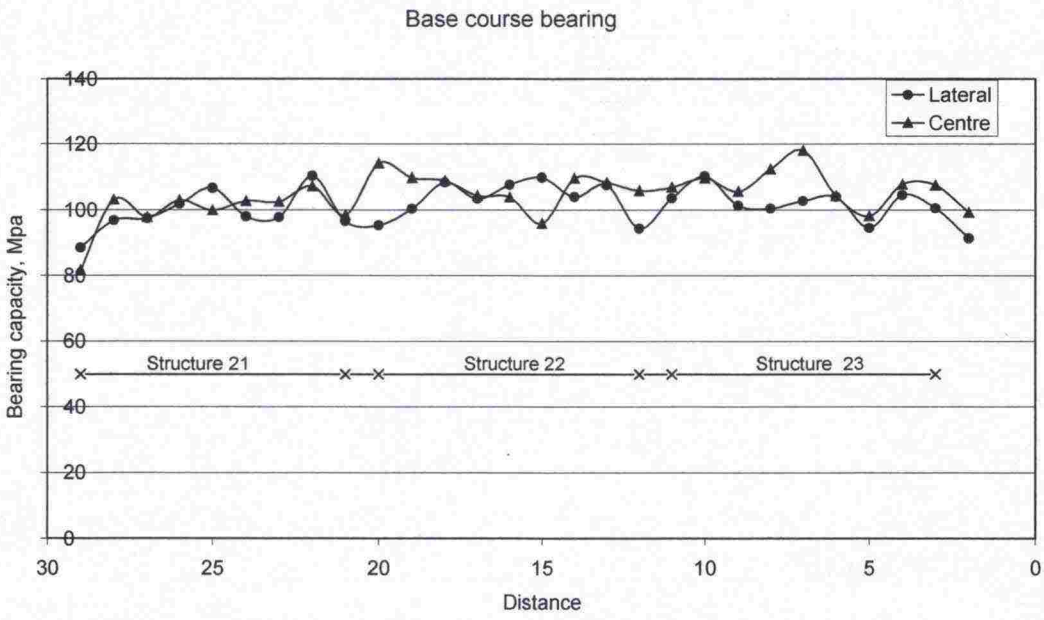

Falling weight deflectometer measurements. Bearing capacity of crushed rock. Lateral line 800 mm right of the centre line.

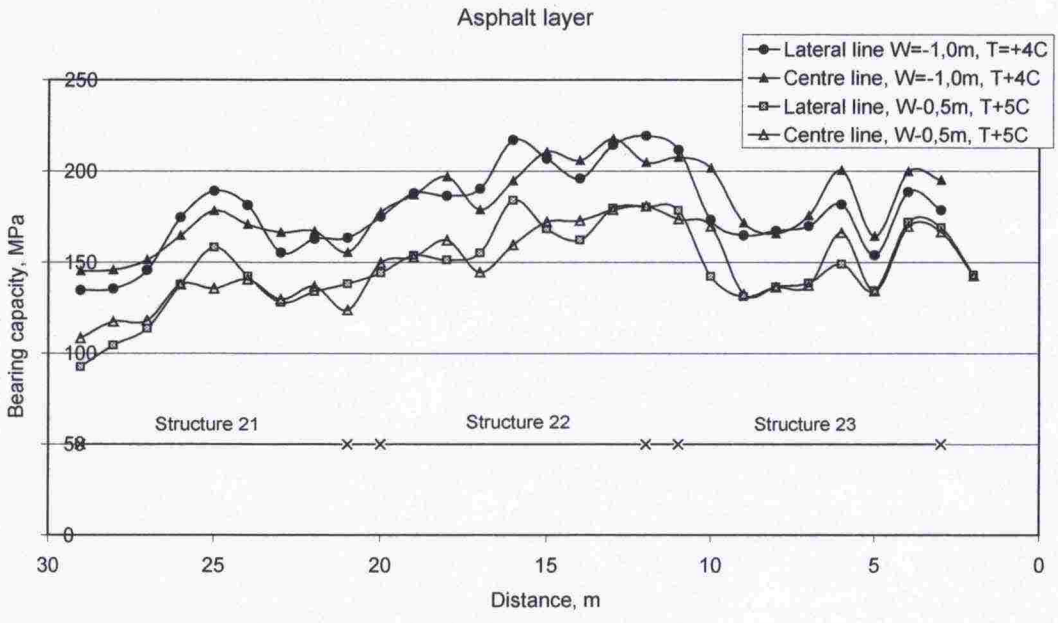

Falling weight deflectometer measurements. Asphalt bearing capacity on different ground water levels (no temperature correction). Lateral line 800 mm right of the centre line.

Falling weight deflectometer measurements. Summary.

E_{FWD}, MPa	Structure 21	Structure 22	Structure 23	Date	Temperature, °C
Crushed gravel, centre	86	98	104	5.2.2002	5
Crushed gravel, lateral	92	99	91	5.2.2002	5
Crushed rock, centre	100	107	108	8.2.2002	5
Crushed rock, lateral	99	103	102	8.2.2002	5
Surf. layer, W–1.0m, centre	161	197	187	18.2.2002	4
Surf. layer, W–1.0m, lateral	160	199	177	18.2.2002	4
Surf. layer, W–0.5m, centre	128	164	154	8.2.2002	5
Surf. layer, W–0.5m, lateral	128	164	150	9.2.2002	5
Surf. layer, W–1.0m, centre after test	206	217	199	11.6.2002	18
Surf. layer, W–1.0m, centre (temp. corr.)	150	180	171	18.2.2002	4 > 20
Surf. layer, W–1.0m, lateral (temp. corr.)	149	182	162	18.2.2002	4 > 20
Surf. layer, W–0.5m, centre (temp. corr.)	119	150	142	8.2.2002	5 > 20
Surf. layer, W–0.5m, lateral (temp. corr.)	119	151	138	9.2.2002	5 > 20
Surf. layer, W–1.0m, lateral after test (temp. corr.)	205	214	196	11.6.2002	18 > 20

APPENDIX 3. LABORATORY RESULTS PROCTOR TESTS.

Sand

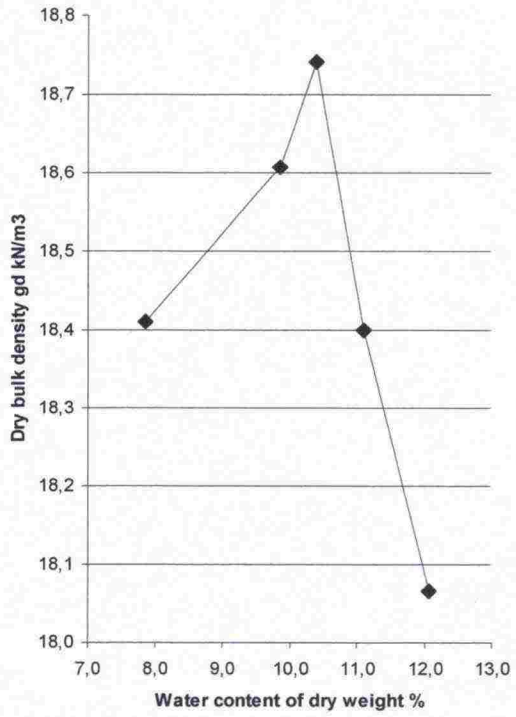

Crushed gravel.

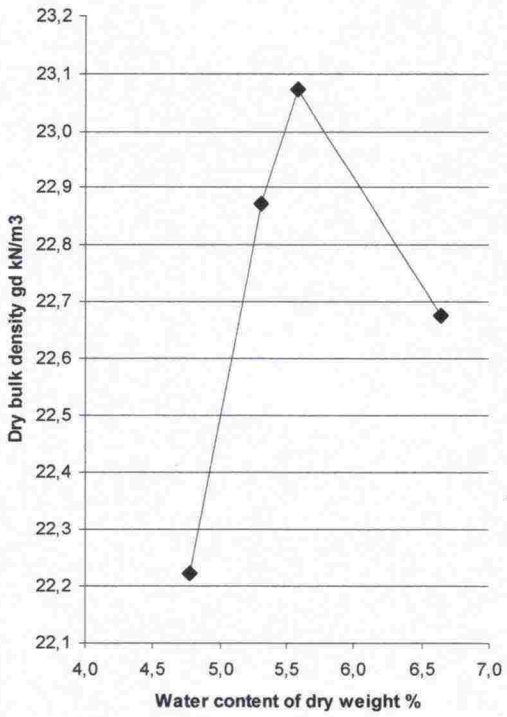

Crushed rock

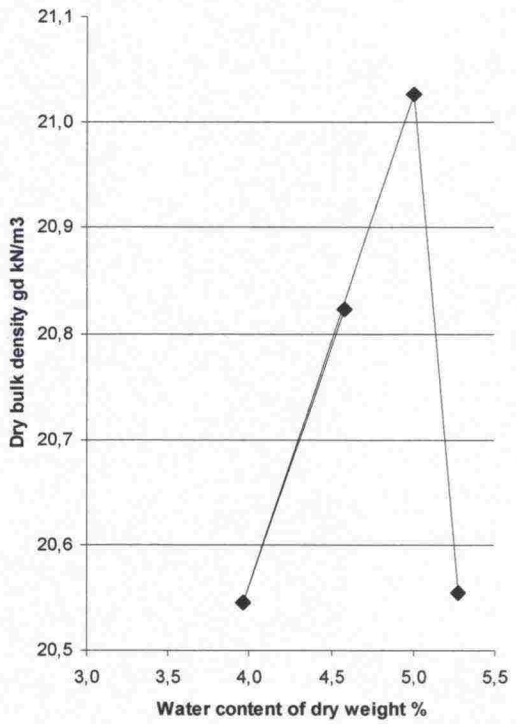

APPENDIX 4. RESULTS OF EARTH PRESSURE MEASUREMENTS.

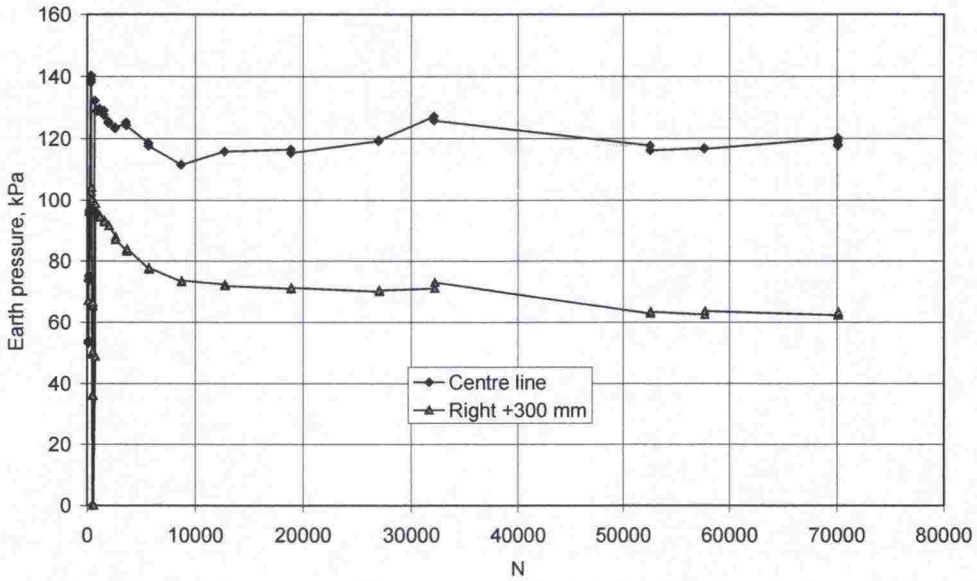

Results of transient earth pressure measurements, structure 21 (70 kN, W -0.5m) sand. The transient earth pressure only includes the increase in earth pressure caused by the loading impulse.

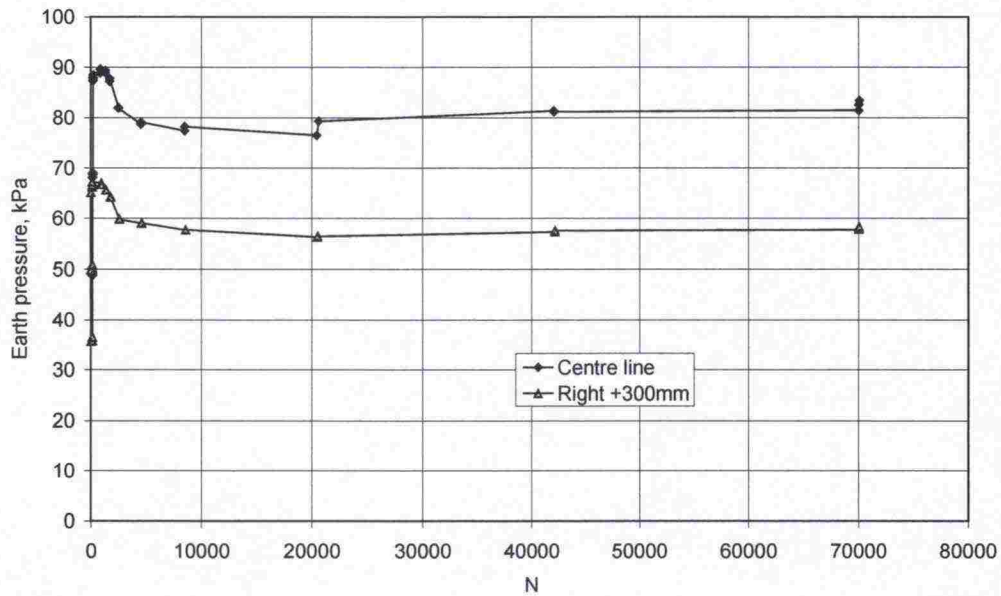

Results of transient earth pressure measurements, structure 22 (50 kN, W -0.5m).

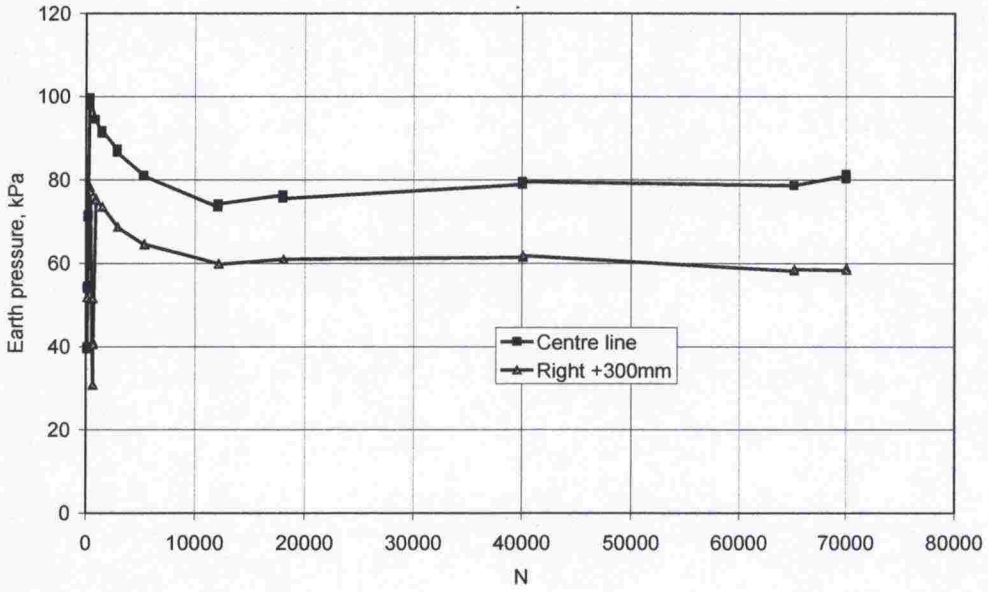

Results of transient earth pressure measurements, structure 23 (70 kN, W -1.0 m).

APPENDIX 5. DEFORMATION MEASUREMENTS.

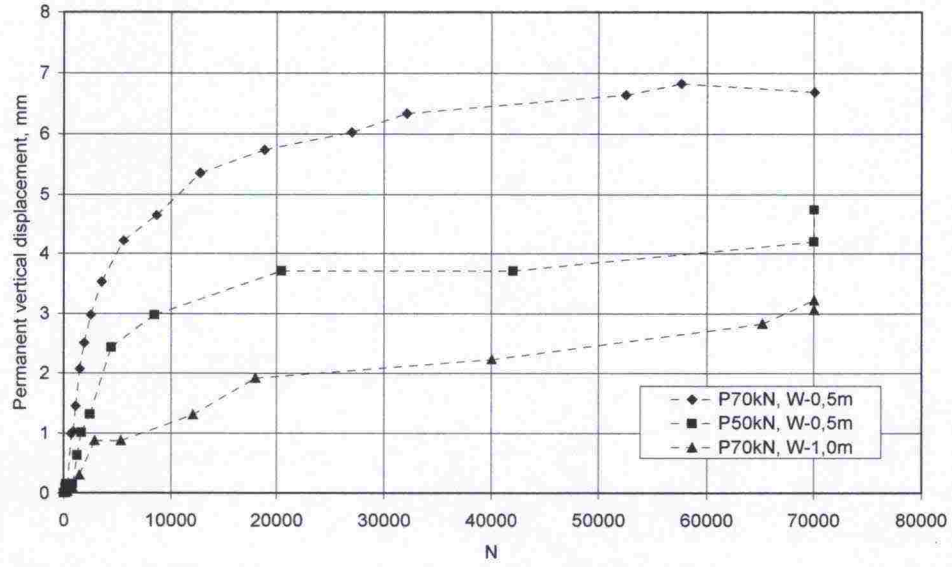

Subgrade sand permanent displacements The distance between Emu-Coil sensors varied between 79.0 and 81.0 mm.

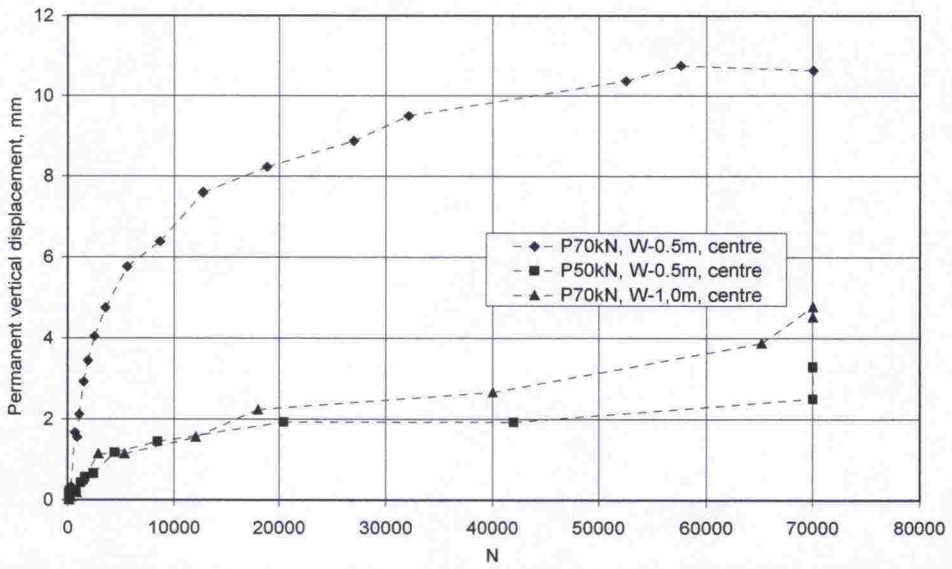

Subbase crushed gravel. Permanent displacements in the centre of the structure. The distance between Emu-Coil sensors varied between 191.3 and 195.2 mm.

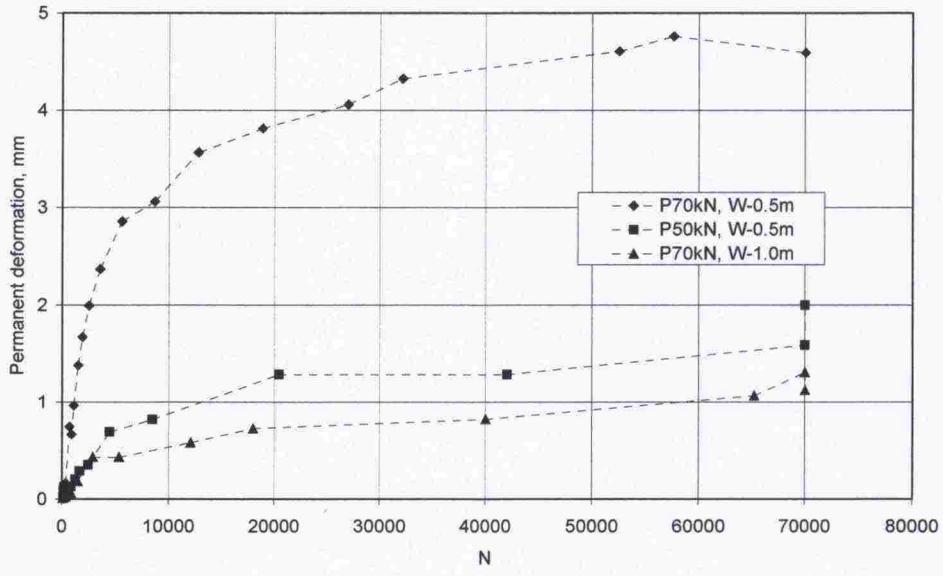

Subbase crushed gravel. Permanent displacements below the loading line, 1 metre from the centre of the structure. The distance between Emu-Coil sensors varied between 72.8 and 79.0 mm.

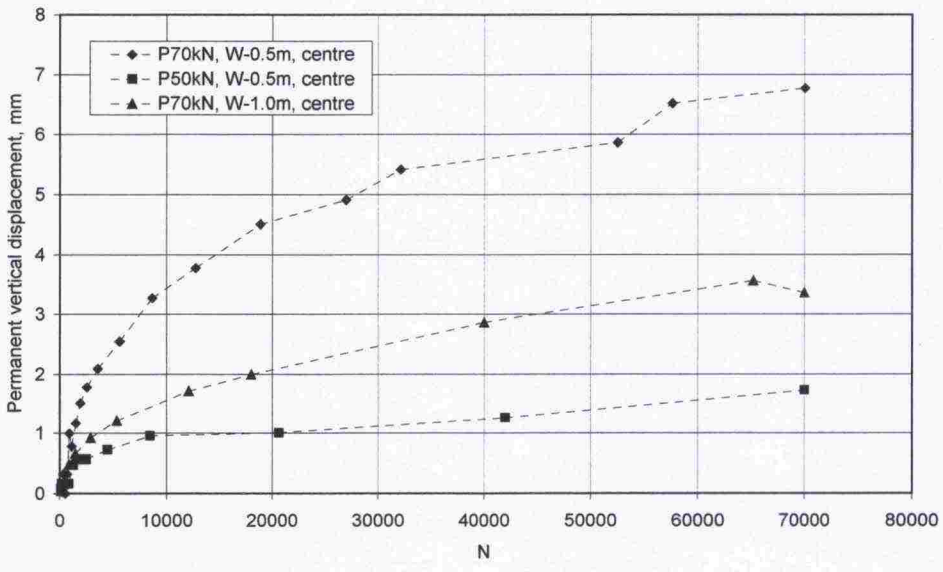

Base course crushed rock. Permanent displacements in the centre of the structure. The distance between Emu-Coil sensors varied between 145.6 and 154.3 mm.

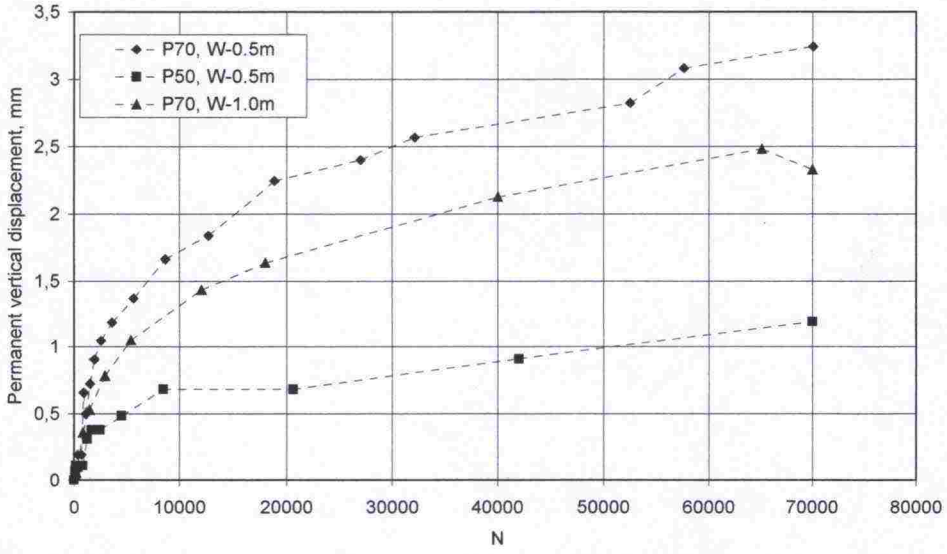

Base course crushed rock. Permanent displacements below the loading line, 1 metre from the centre of the structure. The distance between Emu-Coil sensors varied between 76.5 and 78.7 mm.

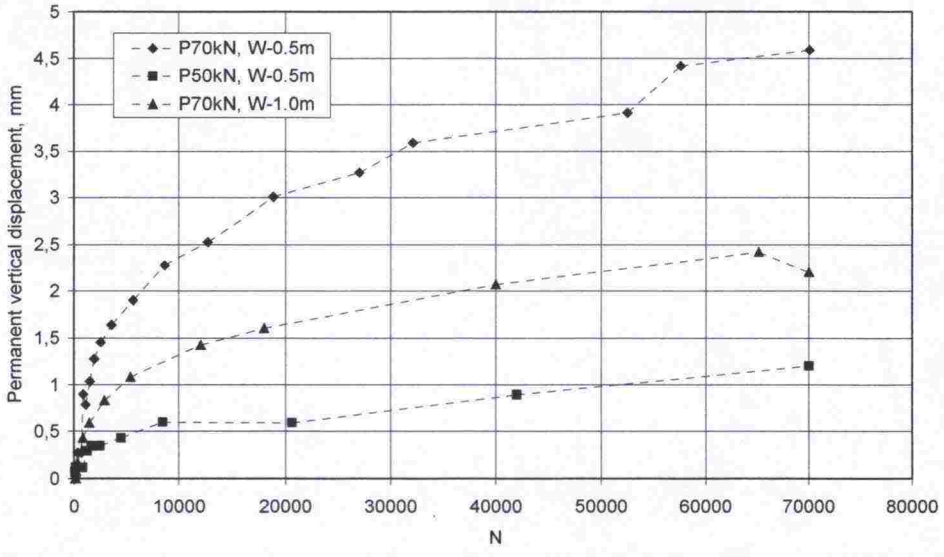

Base course crushed rock. Permanent displacements below the loading line, 2 metres from the centre of the structure. The distance between Emu-Coil sensors varied between 77.1 and 79.6 mm.

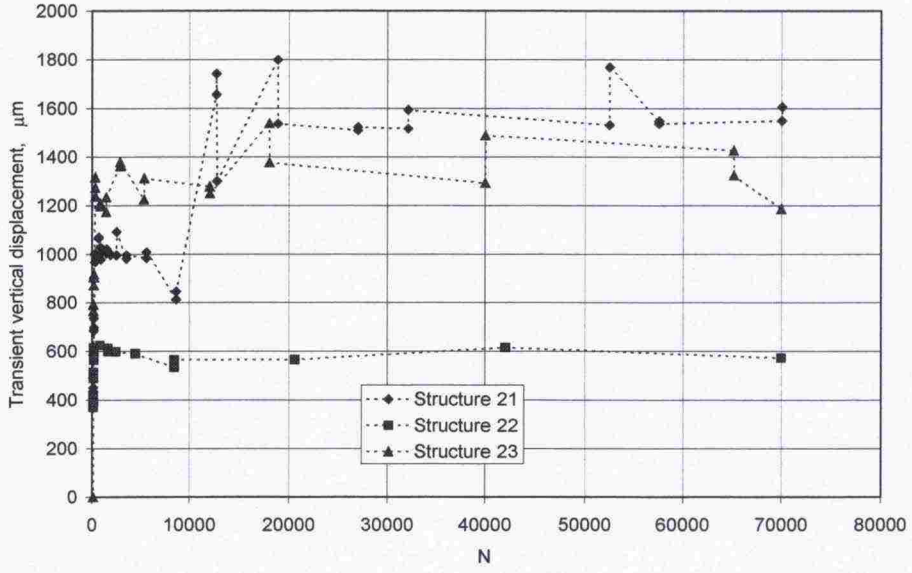

Asphalt transient vertical displacements. Accelerometers.

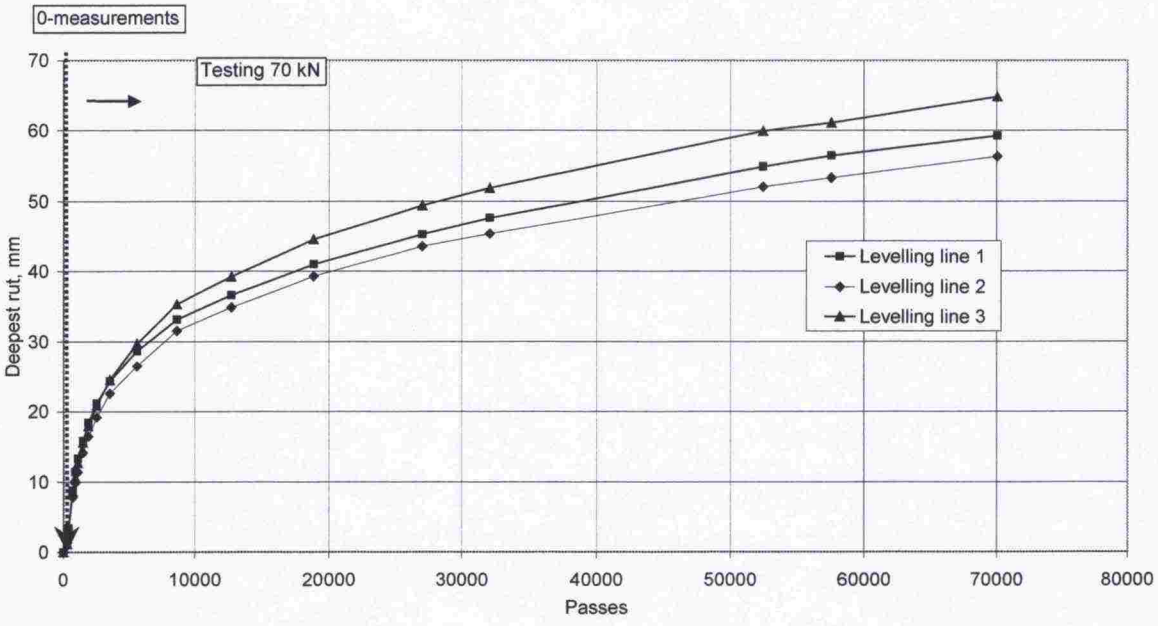

Asphalt rutting.
Profilometer results. Structure 21. Levelling lines 1-3.

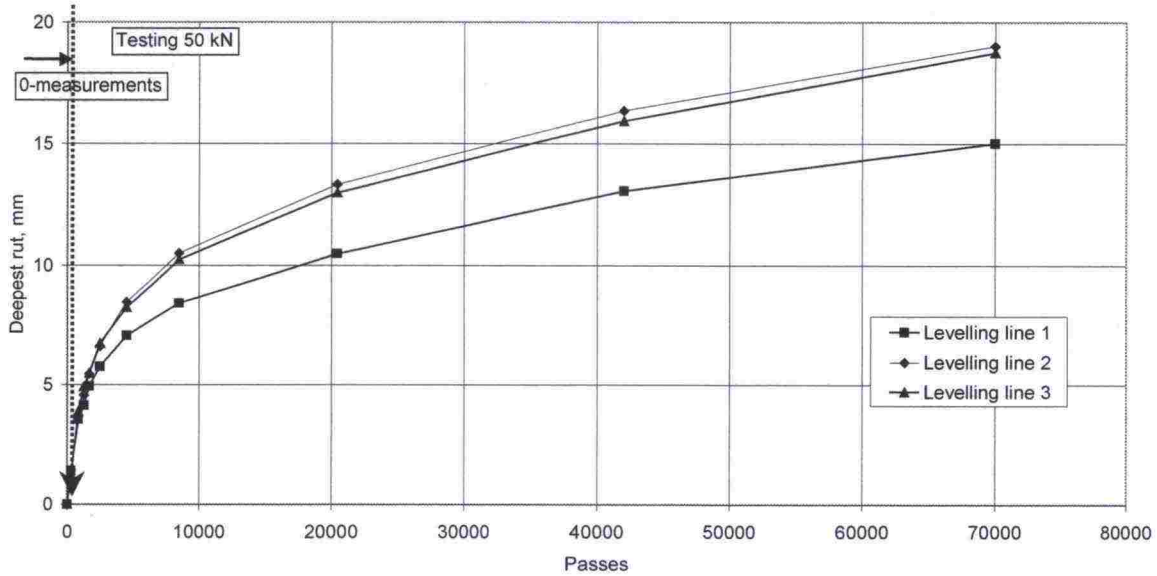

Profilometer results. Structure 22. Levelling lines 1-3.

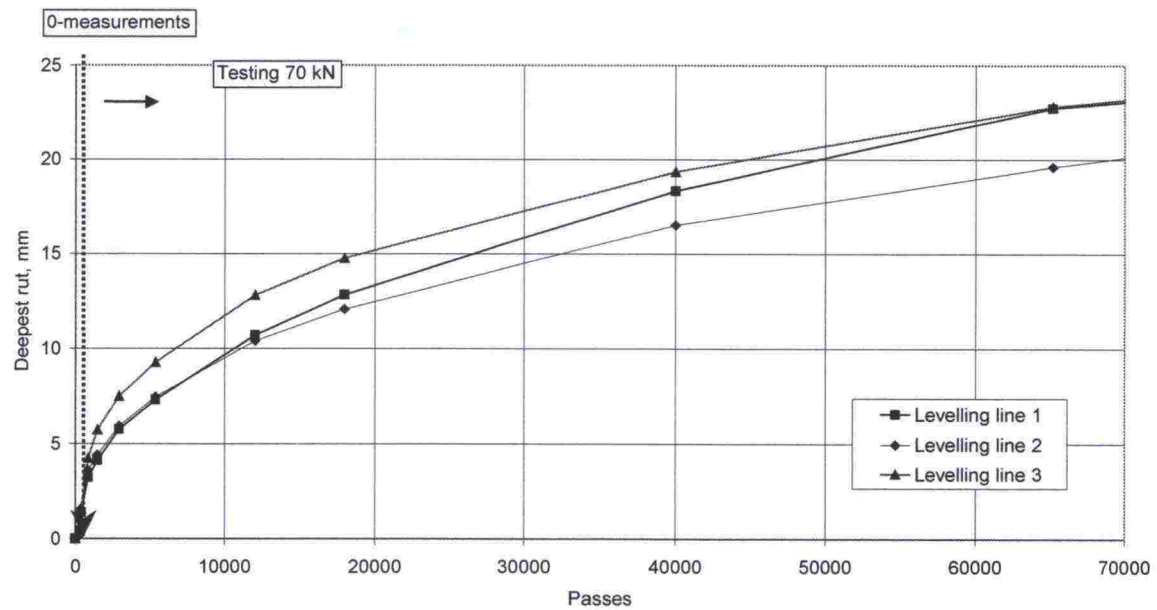

Profilometer results. Structure 23. Levelling lines 1-3.

APPENDIX 6. MEASUREMENTS AFTER LOADING.

Loadman measurements.

E_{132}, Mpa	Structure 21	Structure 22	Structure 23	Date
Asphalt before testing	256	345	325	18.2.2002
Asphalt before testing	248			20.3.2002
Asphalt after preloading	343			21.3.2002
Asphalt after testing	228			28.3.2002
Asphalt before testing		477		5.3.2002
Asphalt after preloading		497		8.3.2002
Asphalt after testing		341		18.3.2002
Asphalt before testing			401	15.4.2002
Asphalt after preloading			368	16.4.2002
Asphalt after testing			274	24.4.2002

*there were cracks on levelling line 1

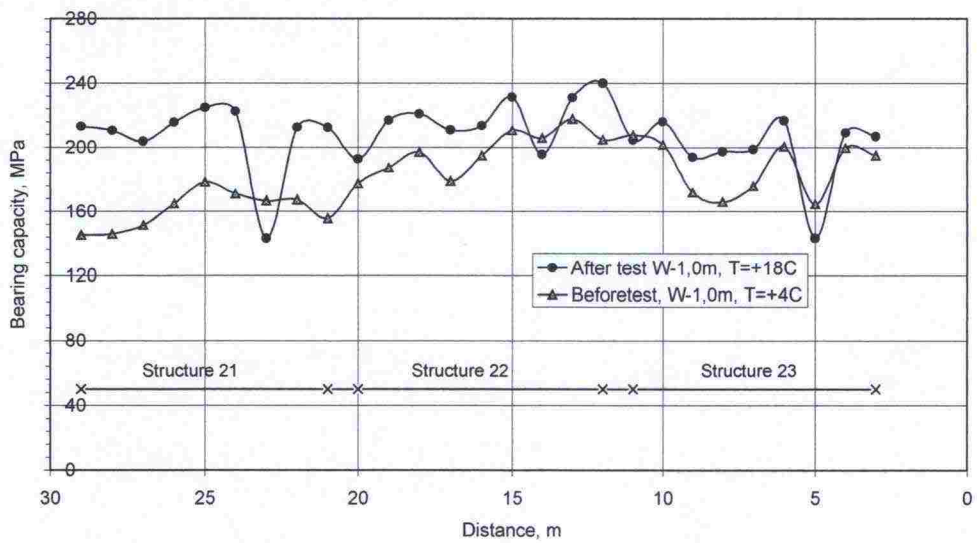

Falling weight deflectometer measurements before testing and after it 11.6.2002.

Density of asphalt according to DOR measurements.

Density, kg/dm3	Structure 21	Structure 22	Structure 23
average	2.301	2.310	2.285
variation	0.035	0.042	0.031

ISSN 1457-9871
ISBN 951-803-052-9
TIEH 3200810E